FEL principle (G8)

Tao Liu (liut@sari.ac.cn)
Shanghai Advanced Research Institute, Chinese Academy of Sciences
OCPA2025, Khao Yai, Nakhon Ratchasima, Thailand, 07.29-08.07, 2025

Lecture Outline

	Time
• Introduction and electron motions in an undulator	14:00-15:00
• Low-gain and high-gain FEL Theory	15:00-16:00
• Break	
• High-gain FEL Analysis and SASE	16:15-17:15
• Seeded FELs	17:15-18:15

Selected references:

- *P. Schmuser, M. Dohlus, and J. Rossbach, Free Electron Lasers in the UV and X-Ray Regime, Springer, 2014*
- *K-J. Kim, Z. Huang, R. Lindberg, Synchrotron Radiation and Free-Electron Lasers, Cambridge University Press, 2017*
- *赵振堂等， 先进X射线光源加速器原理与关键技术，上海交通大学出版社，2017*

Introduction

XFEL: one of the most powerful tools for science

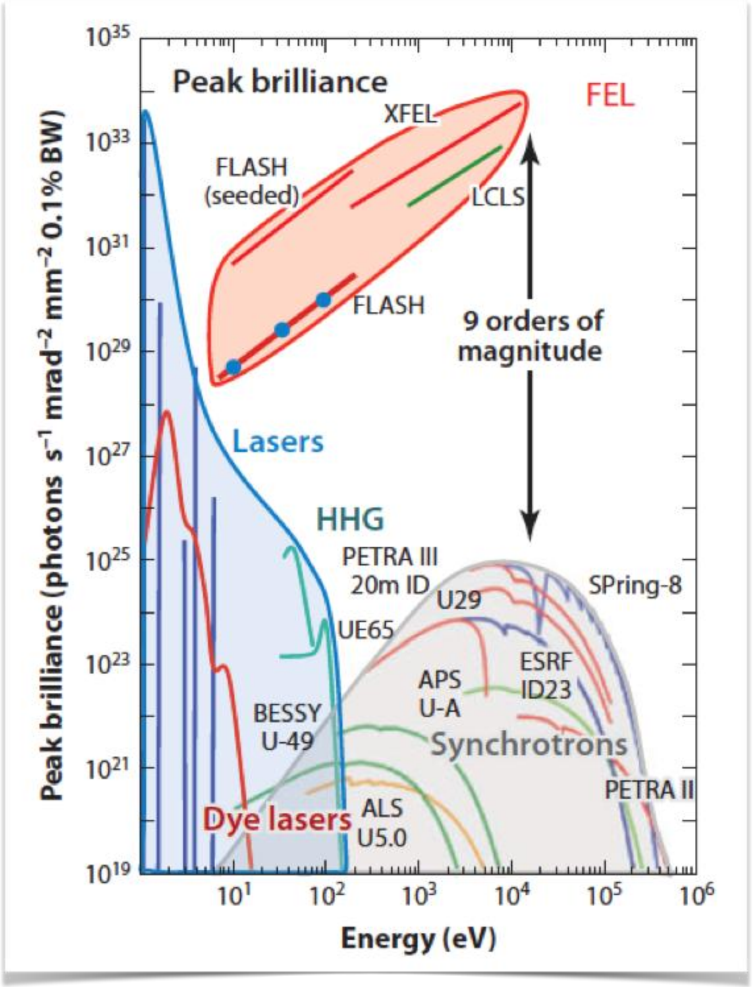

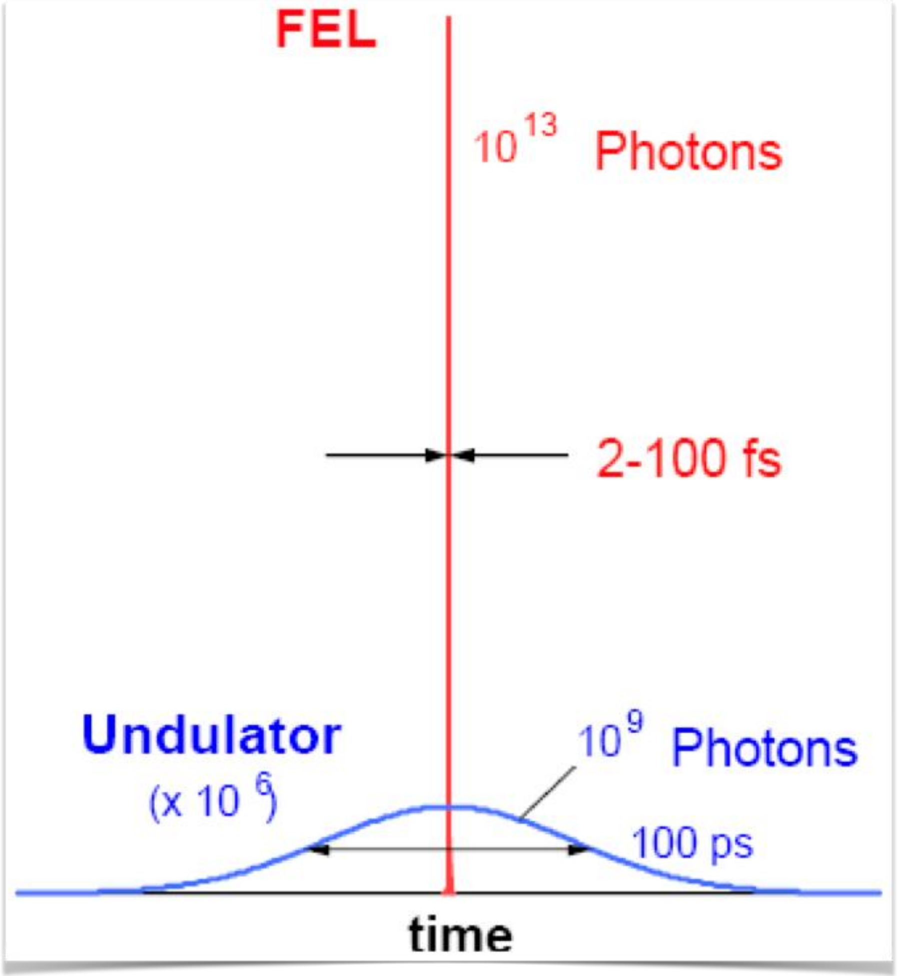

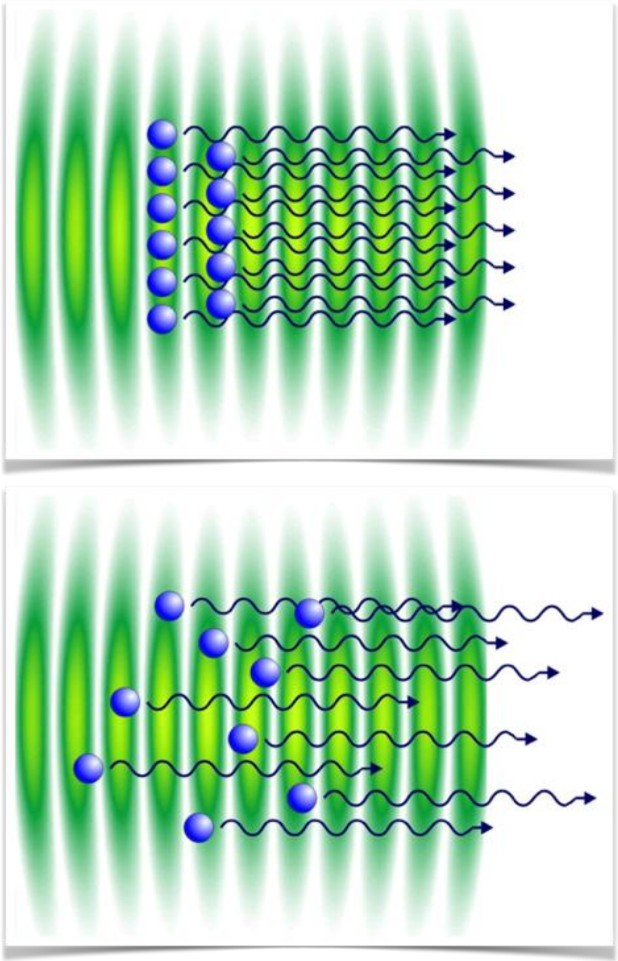

Extremely Bright, Ultrafast, Quasi-Fully Coherence and Wavelength continuous tunability

FEL operation modes

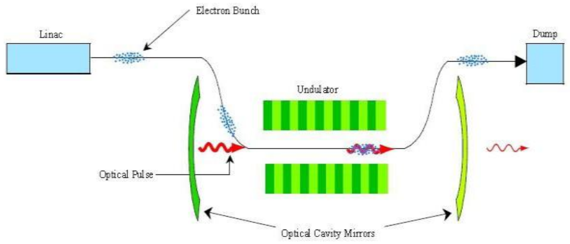

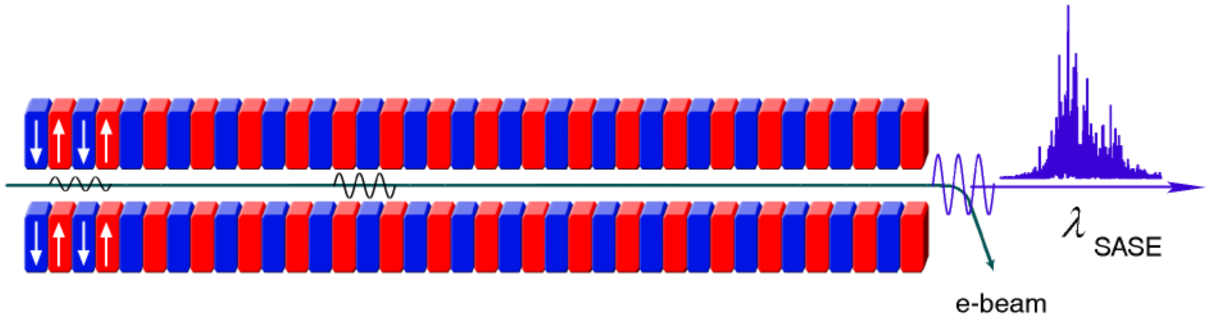

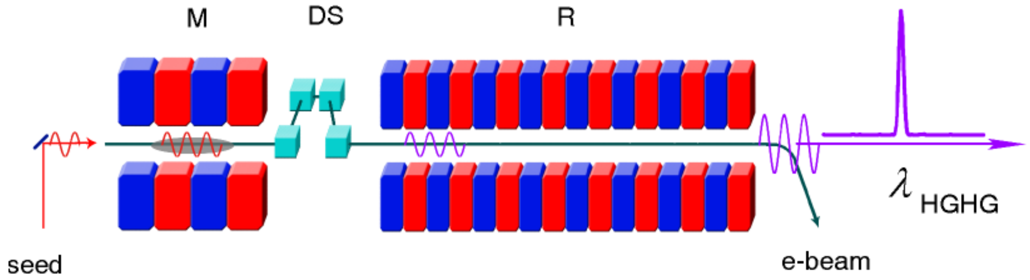

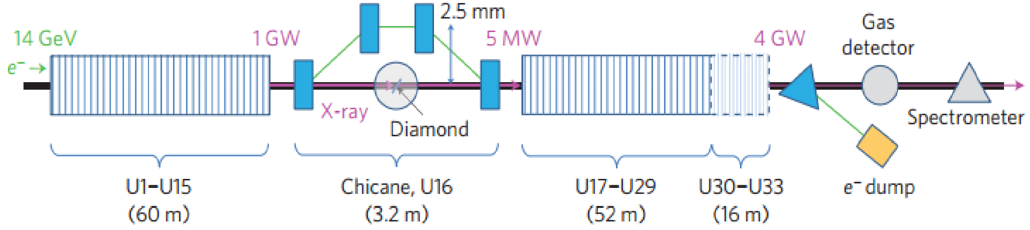

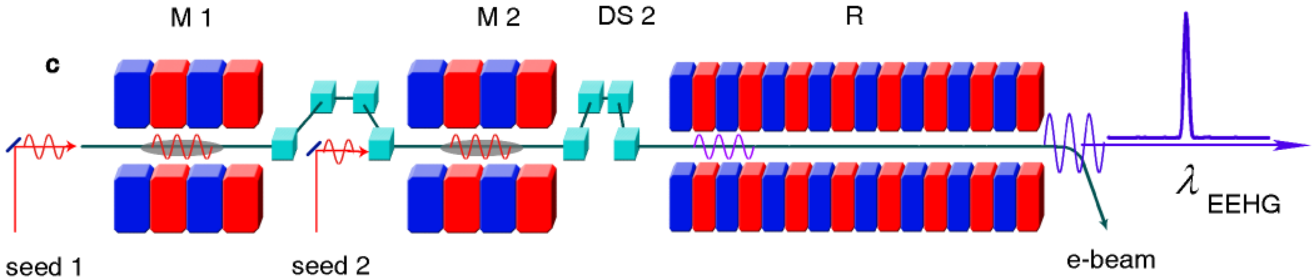

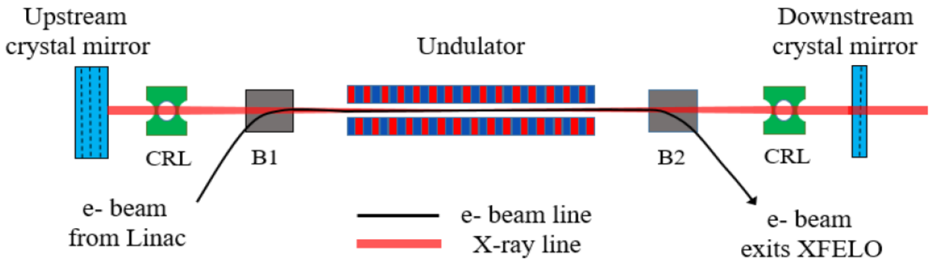

Major Photon Science Centers in the World

Germany
1999
2008

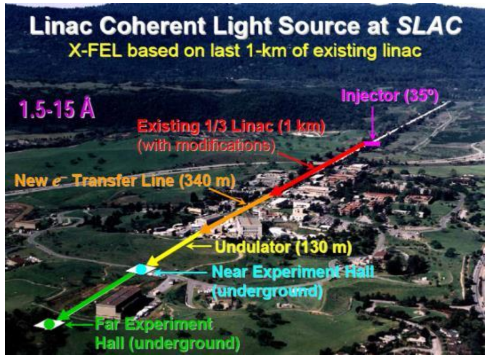

USA
1995
2003

Italy
1994
2007

China
2009
2014

Japan
1997
2006

Switzerland
2001
2010

South Korea
1995
2012

Basic FEL principle

Electron beam ⟷ Interaction ⟷ **Light wave**

Motion equation in undulator ⟷ Energy exchange ⟷ **Electromagnetic field** — Maxwell equation

Stable energy exchange induces resonance condition

- **Electric field evolution**
- **Energy evolution**
- **Particle distribution evolution**

Essential Concepts

- Electron beam
  - Electron energy, relativistic energy factor, relativistic velocity
  - Beam envelope, Twiss parameters, emittance
  - Phase space: transverse and longitudinal
  - Beam transport and optics
- Light
  - Photons: photon energy, wavelength, frequency, wave number
  - Transverse coherence (Diffraction Limit), longitudinal coherence (time-frequency domain, Fourier transform limited)
  - Bunching and intensity enhancement

Bunching and intensity enhancement

- Average electric field intensity generated by electron beam:

$$\left\langle \left| E(\omega) \right|^2 \right\rangle = \left| E_\omega^0 \right|^2 \left\langle \left| \sum_{j=1}^{N_e} e^{i\omega t_j} \right|^2 \right\rangle$$

- Divide the double sum into the piece where the particles are identical and the remaining terms:

$$\left\langle \left| \sum_{j=1}^{N_e} e^{i\omega t_j} \right|^2 \right\rangle = N_e + \left\langle \sum_{j \neq k}^{N_e} e^{i\omega(t_j - t_k)} \right\rangle$$

Incoherent radiation

Coherent FEL emission

$$\left\langle \left| \sum_{j \neq k}^{N_e} e^{i\omega(t_j - t_k)} \right|^2 \right\rangle = N_e(N_e - 1) \left| \int dt\ f(t) e^{i\omega t} \right|^2 = N_e(N_e - 1) \left| f(\omega) \right|^2 .$$

$$f(t) = \frac{1}{\sqrt{2\pi}\,\sigma_e} \exp\left(-\frac{t^2}{2\sigma_e^2} \right) \Rightarrow \left\langle \left| E(\omega) \right|^2 \right\rangle = N_e \left| E_\omega^0 \right|^2 \left[1 + (N_e - 1) e^{-\omega^2 \sigma_e^2} \right]$$

Undulator Radiation Brightness

- Brightness definition：
  - B=(spectral flux)÷(transverse phase space area)
- Undulator Radiation Brightness：

$$\mathcal{B} = \frac{\pi\alpha N_u (I/e)(\Delta\omega/\omega)}{(2\pi\Sigma_x\Sigma_{x'})(2\pi\Sigma_y\Sigma_{y'})}\frac{K^2[JJ]^2}{1+K^2/2}.$$

1. Transverse enhancement: FEL radiation is approximately coherent transversely, so that the phase space area $\Sigma_x\Sigma_{x'}\Sigma_y\Sigma_{y'} \to (\lambda/4\pi)^2$. For 1.5 Å radiation, this gives an enhancement factor over a typical 3$^{\rm rd}$ generation storage ring of

$$\frac{\varepsilon_x\varepsilon_y}{(\lambda/4\pi)^2} \sim \frac{(10^{-9}\text{ m-rad})(10^{-11}\text{ m-rad})(4\pi)^2}{(1.5\times10^{-10}\text{ m-rad})^2} \approx 10^2. \qquad (2.108)$$

2. Temporal enhancement: to achieve the high peak currents required by the FEL process, the bunch length is squeezed by bunch compressors to $\lesssim 100$ fs, which is $\gtrsim 2$ orders of magnitude shorter than that of third-generation sources.
3. Phase-coherence enhancement: in a FEL, electrons in one coherence length radiate together. The intensity enhancement is

$$N_{l_{\rm coh}} = \#\text{ of electrons in one coherence length } l_{\rm coh} \approx 10^6. \qquad (2.109)$$

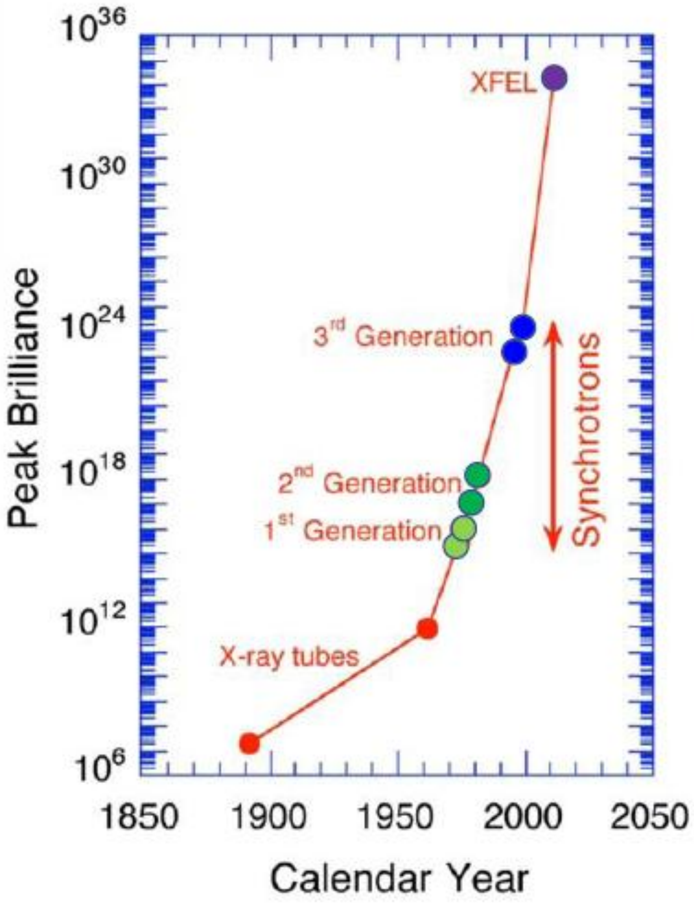

Electron motions in an undulator

Electron trajectory in a planar undulator

Magnetic field in a planar undulator

$$B_x = 0$$
$$B_y = -B_0 \cosh(k_u y) \sin(k_u z)$$
$$B_z = -B_0 \sinh(k_u y) \cos(k_u z)$$

On-axis y=0: $B_y = -B_0 \sin(k_u z)$ for $0 \leq z \leq N_u \lambda_u$

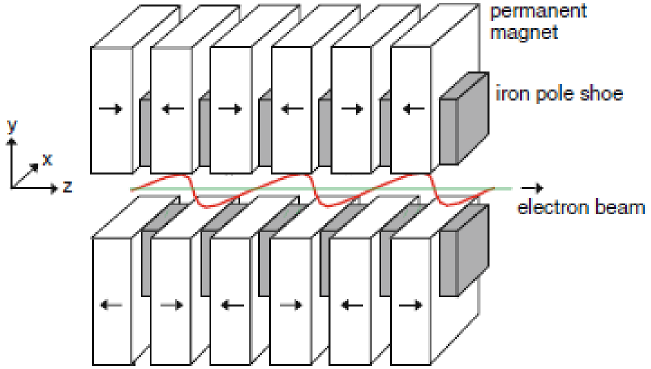

Lorentz force： $\gamma m_e \dot{v} = -ev \times B$

Coupled equations：

$$\ddot{x} = \frac{e}{\gamma m_e} B_y \dot{z} \qquad \ddot{z} = -\frac{e}{\gamma m_e} B_y \dot{x}$$

1st order solution:

$$v_z = \dot{z} \approx v = \beta c = const \text{ and } v_x \ll v_z$$

$$x(t) \approx \frac{eB_0}{\gamma m_e \beta c k_u^2} \sin(k_u \beta c t) , \qquad z(t) \approx \beta c t$$

Transverse motion equations

$$x(z) = \frac{K}{\beta \gamma k_u} \sin(k_u z)$$

$$v_x(z) = \frac{K\, c}{\gamma} \cos(k_u z)$$

$$K = \frac{eB_0}{m_e c k_u} = \frac{eB_0 \lambda_u}{2\pi m_e c} = 0.934 \cdot B_0\,[\mathrm{T}] \cdot \lambda_u\,[\mathrm{cm}] .$$

Undulator parameter K

Electron trajectory in a planar undulator

Due to the sinusoidal trajectory the z component of the velocity is not constant. It is given by

$$v_z = \sqrt{v^2 - v_x^2} \approx c\left(1 - \frac{1}{2\gamma^2}\left(1 + \gamma^2 v_x^2/c^2\right)\right) .$$

Inserting for $v_x = \dot{x}(t)$ the first-order solution, the z velocity becomes

$$v_z(t) = \left(1 - \frac{1}{2\gamma^2}\left(1 + \frac{K^2}{2}\right)\right) c - \frac{cK^2}{4\gamma^2}\cos(2\omega_u t) \qquad (2.12)$$

with the abbreviation $\omega_u = \bar{\beta} c k_u$. The average longitudinal speed is

$$\boxed{\bar{v}_z = \left(1 - \frac{1}{2\gamma^2}\left(1 + \frac{K^2}{2}\right)\right) c \equiv \bar{\beta}\, c\, .} \qquad (2.13)$$

In beam frame

The particle trajectory in second order is described by the equations

$$\boxed{x(t) = \frac{K}{\gamma k_u}\sin(\omega_u t)\, , \qquad z(t) = \bar{v}_z t - \frac{K^2}{8\gamma^2 k_u}\sin(2\omega_u t)\, .} \qquad (2.14)$$

8

Undulator radiation resonant wavelength

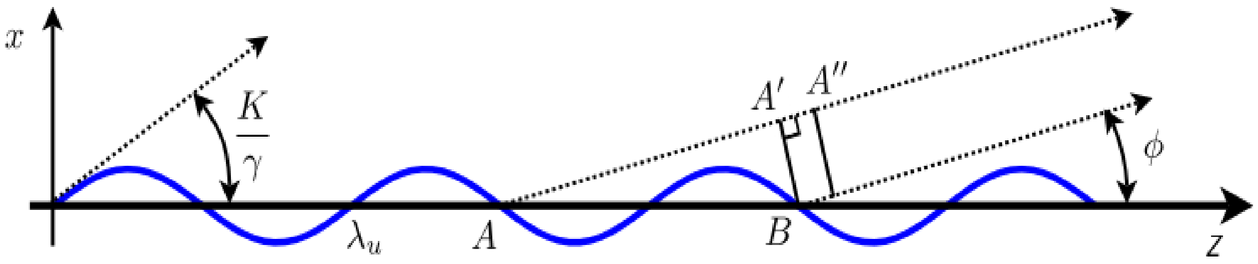

$$\frac{\lambda_1(\phi)}{c} = \frac{\widetilde{AB}}{v} - \frac{\overline{AA'}}{c}$$

$$\widetilde{AB} = \int_0^{\lambda_u} dz\, \sqrt{1+(x')^2} \approx \int_0^{\lambda_u} dz\, \left(1+\frac{1}{2}x'^2\right) = \lambda_u\left(1+\frac{K^2}{4\gamma^2}\right)$$

$$\overline{AA'} = \lambda_u \cos\phi \approx \lambda_u\left(1-\frac{\phi^2}{2}\right)$$

$$\frac{\lambda_1(\phi)}{c} = \frac{\lambda_u}{c}\left[\frac{1+K^2/(4\gamma^2)}{\beta} - \left(1-\frac{\phi^2}{2}\right)\right]$$

$$\approx \frac{\lambda_u}{c}\frac{1+K^2/2+\gamma^2\phi^2}{2\gamma^2},$$

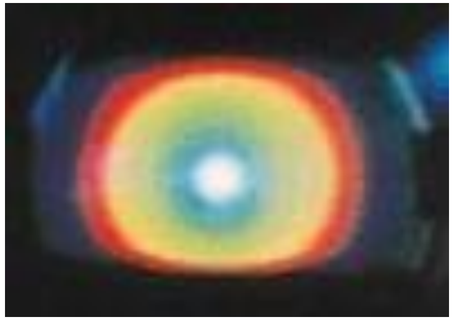

UVSOR, Okazaki, Japan

Works for harmonics $\lambda_h=\lambda_1/h$

Radiation spectrum

Since any electron makes N_u oscillations in an undulator composed of N_u periods, the resulting wave train has N_u cycles. Thus, the spectrum of the undulator radiation at observation angle ϕ is peaked around $\omega_1(\phi)$ with intrinsic bandwidth

$$\boxed{\frac{\Delta\omega}{\omega_1} = \frac{\Delta\lambda}{\lambda_1} \sim \frac{1}{N_u}.}$$

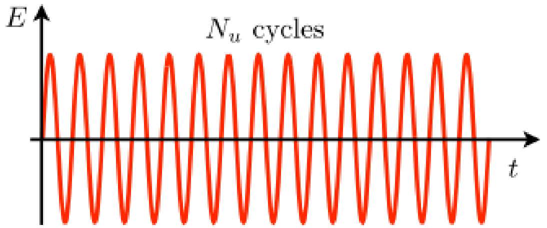

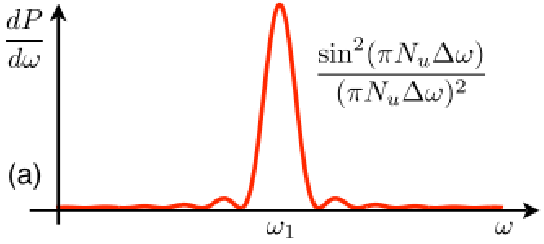

$$E_l(t) = \begin{cases} E_0 e^{-i\omega_1 t} & if -\frac{T}{2} < t < \frac{T}{2} \\ 0 & \text{otherwise} \end{cases} \qquad T = N_u \lambda_u / C$$

$$A(\omega) = \int_{-\infty}^{+\infty} E_\ell(t) e^{i\omega t} dt = E_0 \int_{-T/2}^{+T/2} e^{-i(\omega_1 - \omega)t} dt$$

$$= 2E_0 \cdot \frac{\sin((\omega_1 - \omega)T/2)}{\omega_1 - \omega} .$$

The spectral intensity is

$$I(\omega) \propto |A(\omega)|^2 \propto \left(\frac{\sin \xi}{\xi}\right)^2 \quad \text{with} \quad \xi = \frac{(\omega_1 - \omega)T}{2} = \pi N_u \frac{\omega_1 - \omega}{\omega_1} .$$

It has a maximum at $\omega = \omega_1$ and a full width at half maximum of

$$\Delta\omega \approx \frac{\omega_1}{N_u} .$$

Radiation angular divergence

$$\frac{\lambda_1(\phi)-\lambda_1(0)}{\lambda_1(0)}=\frac{\gamma^2\phi^2}{1+K^2/2}=\frac{\lambda_u}{2\lambda_1(0)}\phi^2>0.$$

1）$\Phi \sim 1/\gamma$，large bandwidth (bending)
2）$\Phi << 1/\gamma$，observe intrinsic bandwidth

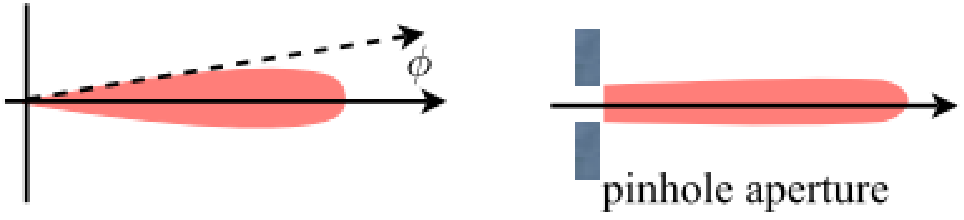

Observing the intrinsic bandwidth to obtain the natural divergence of undulator radiation

$$\frac{\Delta\lambda}{\lambda}=\frac{\gamma^2\phi^2}{1+K^2/2}=\frac{\lambda_u}{2\lambda_1(0)}(\Delta\phi)^2\leq\frac{1}{N_u}.$$

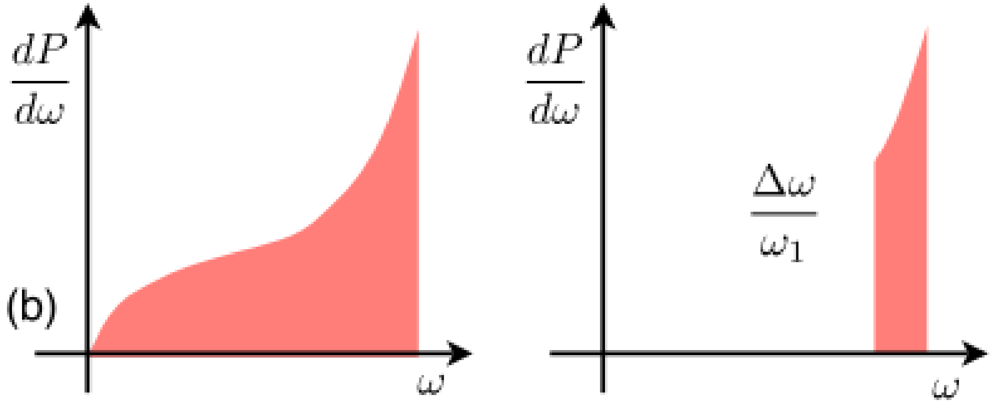

Defining rms angular divergence $\sigma_{r'}\equiv\Delta\phi/2.$

$$\Delta\phi\leq\frac{1}{\gamma}\sqrt{\frac{1+K^2/2}{N_u}} \Rightarrow \sigma_{r'}=\sqrt{\frac{\lambda_1}{2L_u}}\approx\frac{1}{\gamma}\cdot\frac{1}{\sqrt{N_u}}$$

Higher harmonics

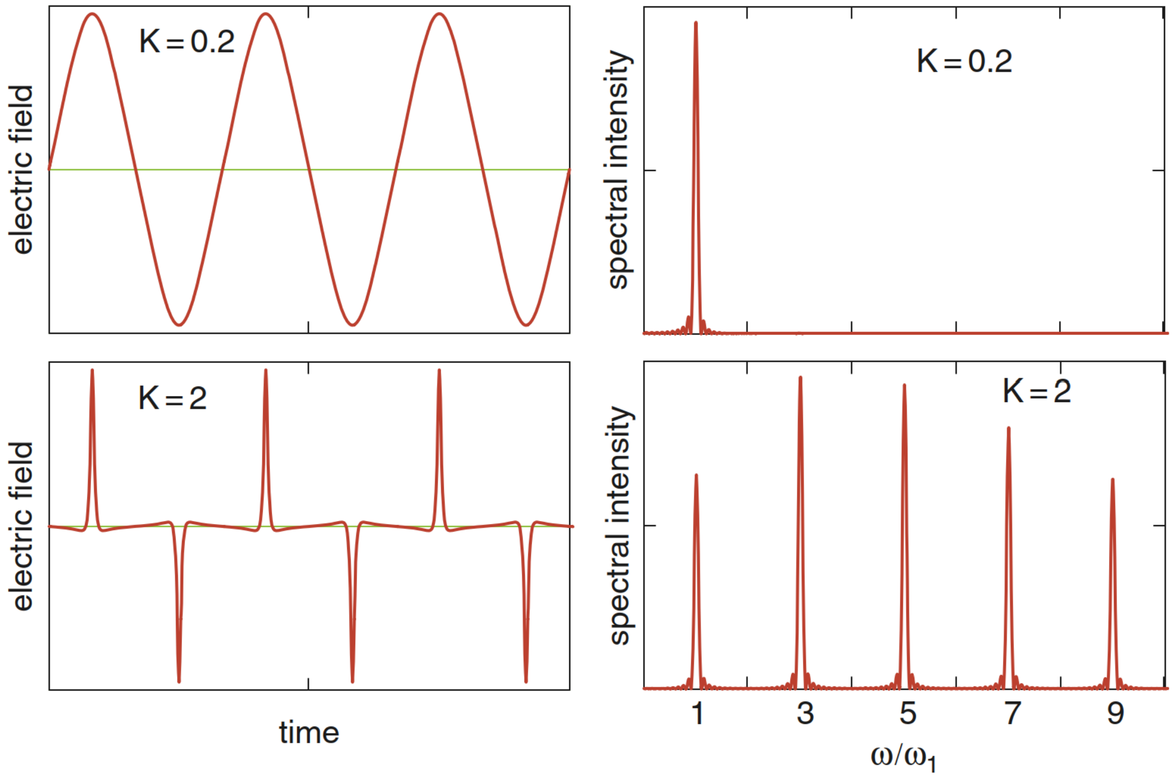

The wavelength of the mth harmonic as a function of the angle θ is

$$\lambda_m(\theta) = \frac{1}{m}\frac{\lambda_u}{2\gamma^2}\left(1 + K^2/2 + \gamma^2\theta^2\right), \quad m = 1,\ 2,\ 3,\ 4, \dots . \qquad (2.28)$$

In forward direction only the odd harmonics are observed with the wavelengths

$$\boxed{\lambda_m = \frac{1}{m}\frac{\lambda_u}{2\gamma^2}\left(1 + K^2/2\right), \quad m = 1,\ 3,\ 5, \dots} \qquad (2.29)$$

The absolute bandwidth at $\theta = 0$ is the same for all harmonics

$$\Delta\omega_1 = \Delta\omega_3 = \Delta\omega_5 \dots$$

but the fractional bandwidth drops as $1/m$

$$\frac{\Delta\omega_m}{\omega_m} = \frac{1}{mN_u} \qquad (2.31)$$

because the wave train comprises now mN_u oscillations in an undulator with N_u periods. The angular width is [4]

$$\sigma_{\theta,\,m} \approx \frac{1}{\gamma}\cdot\sqrt{\frac{1 + K^2/2}{2mN_u}} \approx \frac{1}{\gamma}\cdot\frac{1}{\sqrt{mN_u}} \quad \text{for} \quad K \approx 1 . \qquad (2.32)$$

The corresponding solid angle

$$\Delta\Omega_m = 2\pi\sigma^2_{\theta,\,m} \approx \frac{2\pi}{\gamma^2}\cdot\frac{1}{m\,N_u}$$

Interaction and energy exchange

- **Energy exchange:** coupling between electron transverse velocity and transverse electric field; continuous energy transfer.

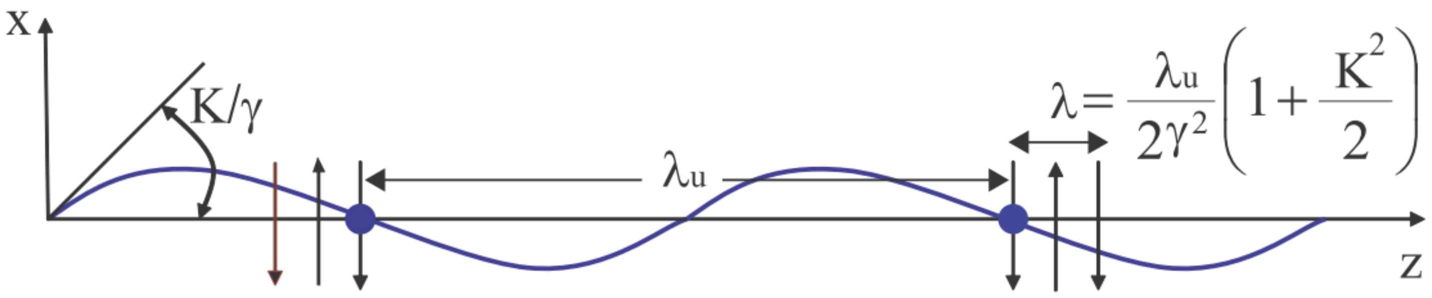

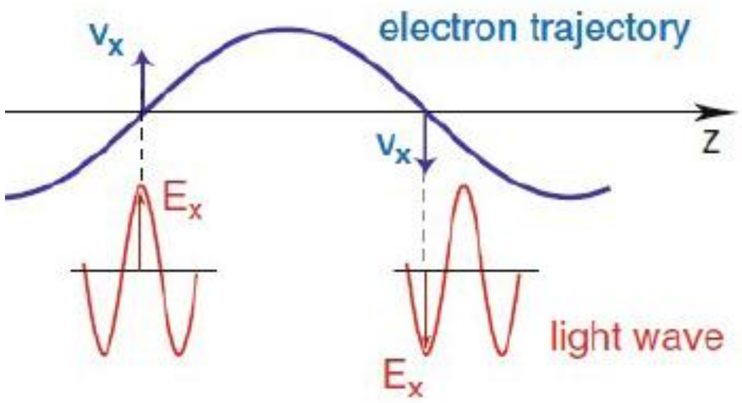

电子与光场在纵向上的“滑移效应”（slippage）使光场获得持续增益，滑移长度：$L_{slip} = N_u\lambda_s$

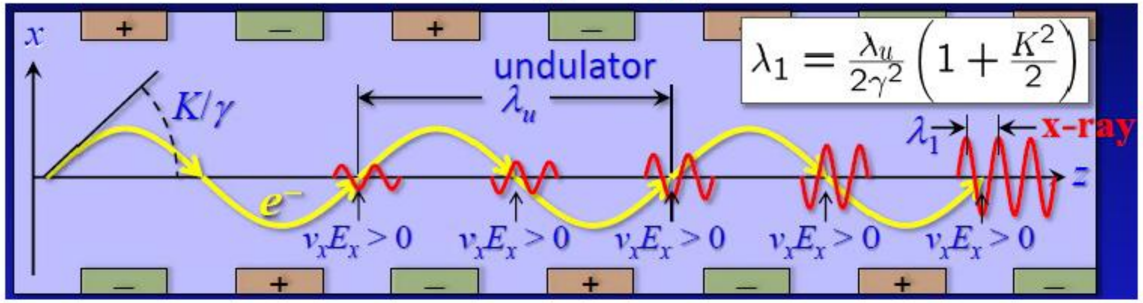

Interaction and energy exchange

- Energy transfer（Power）

$$\frac{dW}{dt} = \boldsymbol{v} \cdot \boldsymbol{F} = -ev_x(t)E_x(t)$$

$$v_x = \frac{Kc}{\gamma}\cos(k_u z)$$

$$\boldsymbol{E}(z,t) = \hat{x}E_0 \sin(kz - \omega t + \phi), \qquad \omega = ck = \frac{2\pi c}{\lambda}.$$

$$\boldsymbol{F} \cdot \boldsymbol{v} = -e\boldsymbol{E} \cdot \boldsymbol{v} = -\frac{eE_0 Kc}{\gamma}\cos(k_u z)\sin(kz - \omega t + \phi) \neq 0$$

$F \cdot v > 0$, inverse FEL $\qquad$ $F \cdot v < 0$, FEL

Interaction and energy exchange

- The time derivative of the electron energy

$$\frac{d\gamma}{dt} = -\frac{eE_0Kc}{mc^2\gamma}\cos(k_u z)\sin(kz - \omega t + \phi)$$
$$= -\frac{eE_0Kc}{2mc^2\gamma}\left\{\underbrace{\sin\left[(k+k_u)z - \omega t + \phi\right]}_{\sim \text{particle phase } \theta} + \underbrace{\sin\left[(k-k_u)z - \omega t + \phi\right]}_{\text{neglect, will justify later}}\right\}$$

where we have introduced the particle phase $\theta \equiv (k + k_u)z - \omega t + \phi$

The time derivative of the particle phase:

the ponderomotive phase

$$\frac{d\theta}{dt} = (k + k_u)v_z - ck. \qquad v_z \to \bar{v}_z = c\left(1 - \frac{1 + K^2/2}{2\gamma^2}\right)$$

$$\frac{d\theta}{dt} = ck\left(\frac{k_u}{k} - \frac{1 + K^2/2}{2\gamma^2}\right)$$

Interaction and energy exchange

In order to have a stationary phase ($d\theta/dt = 0$) and significant energy exchange, we need

$$\frac{k_u}{k} = \frac{\lambda}{\lambda_u} = \frac{1 + K^2/2}{2\gamma^2}, \tag{4.8}$$

This is resonant condition if $\lambda = \lambda_1$, and $\gamma = \gamma_r$

$$\boxed{\lambda_\ell = \frac{\lambda_u}{2\gamma_r^2}\left(1 + \frac{K^2}{2}\right) \quad \Rightarrow \quad \gamma_r = \sqrt{\frac{\lambda_u}{2\lambda_\ell}\left(1 + \frac{K^2}{2}\right)}\,.}$$

Since γ a function of time, we introduce a normalized energy variable

$$\eta \equiv \frac{\gamma - \gamma_r}{\gamma_r} \ll 1$$

Due to the interaction between electrons and radiation fields, both the electron energy γ and the ponderomotive phase θ undergo evolution. In the low gain FEL theory, the amplitude of the electric field can be treated as a constant in a short undulator due to its slow growth.

Interaction and energy exchange

The coupled phase-energy equations

$$\frac{d\theta_j}{dt} = 2k_u c\eta_j \qquad \frac{d\eta_j}{dt} = \frac{1}{\gamma_r}\frac{d\gamma_j}{dt} = -\frac{eE_0Kc}{2\gamma_j\gamma_r mc^2}\sin\theta_j .$$

(j for each individual electron)

It is convenient to use z as the independent variable $z \sim ct$

z: The independent variable giving the location inside the undulator.

$t(z)$: The time an electron arrives at z.

$\theta(z)$: The ponderomotive phase defined by

$$\theta = (k+k_u)z - \omega t + \text{const.} = \omega\left[\frac{k+k_u}{\omega}z - \bar{t}(z)\right] + \text{const.}$$
$$= \omega\left[z/\bar{v}_z - \bar{t}(z)\right] + \text{const.} \qquad (4.21)$$

If we keep track of the oscillatory part of $v_z = \bar{v}_z - \frac{cK^2}{4\gamma^2}\cos(2k_u z) \approx \bar{v}_z - \frac{ck_u K^2}{k_1(2+K^2)}\cos(2k_u z)$

$$K \longrightarrow K[\text{JJ}], \quad \text{with} \quad [\text{JJ}] \equiv J_0\left(\frac{K^2}{4+2K^2}\right) - J_1\left(\frac{K^2}{4+2K^2}\right)$$

FEL Pendulum equation

The Hamiltonian form of the low-gain FEL:

$$H = k_u \eta^2 - \frac{\epsilon}{2k_u L_u^2} \cos\theta\,. \qquad \dot{\theta} = \frac{\partial H}{\partial \eta} = 2k_u\eta, \quad \dot{\eta} = -\frac{\partial H}{\partial \theta} = -\frac{\epsilon}{2k_u L_u^2}\sin\theta \qquad \epsilon = \frac{eE_0 K[\mathrm{JJ}]}{\gamma_r^2 mc^2} k_u L_u^2$$

The trajectories in the (θ, η) phase space are the curves of a constant *H with the separatrices joining the two unstable points at* (θ=$\pm\pi$, η=0)

$$\eta = \pm\frac{\sqrt{\epsilon}}{k_u L_u}\sqrt{(1+\cos\theta)/2} = \pm\frac{\sqrt{\epsilon}}{k_u L_u}\cos(\theta/2).$$

Approximately written as a 2nd order equation

$$d^2\theta/dz^2 = -k_s^2\theta.$$

The natural oscillation frequency is given by

$$k_s = \frac{\sqrt{\epsilon}}{L_u} = \sqrt{\frac{eE_0 K[\mathrm{JJ}] k_u}{\gamma_r^2 mc^2}}$$ with period $z_s \equiv \frac{2\pi}{k_s}$.

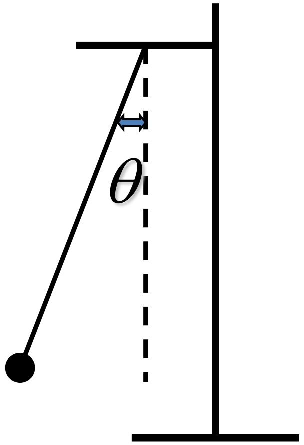

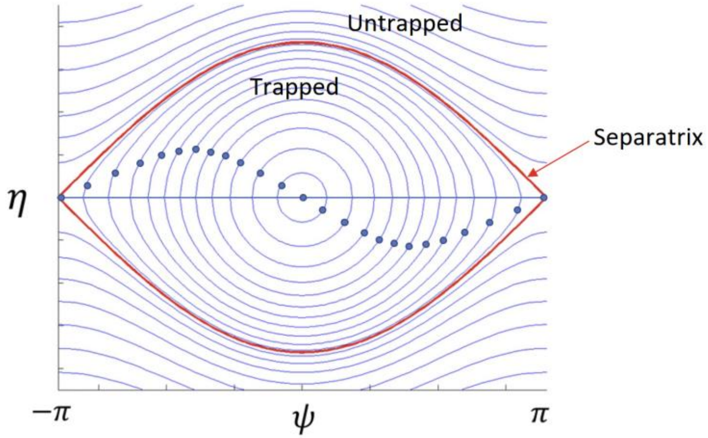

FEL bucket

Low gain FEL theory
(Small-signal gain)

Low-gain regime

In addition, we simplify the analysis by solving for the electron motion perturbatively under the assumption that the electrons do not significantly rotate in the pendulum potential. This assumption is equivalent to assuming that the synchrotron period times the undulator length is small, or that the dimensionless field strength $\epsilon \equiv (\Omega_s L_u)^2 \ll 1$. We then develop the perturbation equations by expanding the phase space variables as

$$\theta = \theta_0(z) + \epsilon\theta_1(z) + \epsilon^2\theta_2(z) + \dots$$

$$\eta = \eta_0(z) + \epsilon\eta_1(z) + \epsilon^2\eta_2(z) + \dots .$$

Recall the phase & energy equation

$$\frac{d\theta}{dz} = 2k_u\eta, \qquad \frac{d\eta}{dz} = -\frac{\epsilon}{2k_u L_u^2}\sin\theta.$$

We will solve the pendulum equations in the low-gain regime where the amplification in a single-pass of the undulator is small, so that $\varepsilon \approx$ constant.

Low-gain regime

Inserting the expansion into the equations of motion, yields

$$\frac{d\theta_m}{dz} = 2k_u\eta_m,$$

$$\frac{d\eta_0}{dz} + \epsilon\frac{d\eta_1}{dz} + \epsilon^2\frac{d\eta_2}{dz} = -\frac{\epsilon}{2k_uL_u^2}(\sin\theta_0 + \epsilon\theta_1\cos\theta_0),$$

3 phase equations
3 energy equations

Then, at **0-th order**, we have

$$\frac{d\eta_0}{dz} = 0 \qquad \frac{d\theta_0}{dz} = 2k_u\eta_0$$

$$\Rightarrow \eta_0 = \text{const} \qquad \Rightarrow \theta_0(z) = 2k_u\eta_0 z + \phi_0,$$

with (φ_0, η_0) defined to be the initial particle coordinates in phase space.
At lowest order the particles move in straight lines with constant velocity.

Low-gain regime

The interaction with the field comes in with the first-order equations

$$\frac{d\theta_1}{dz} = 2k_u\eta_1,$$
$$\frac{d\eta_1}{dz} = -\frac{1}{2k_u L_u^2}\sin\theta_0 .$$

Putting the 0-th order solutions into above equation, and solving for η_1, we have

$$\eta_1(z) = -\frac{1}{2k_u L_u^2}\int_0^z dz'\ \sin\theta_0(z') = \frac{\cos\theta_0(z) - \cos\phi_0}{4k_u^2 L_u^2 \eta_0} .$$

$\theta_0(z) = 2k_u\eta_0 z + \phi_0$

Note that the average of the **first-order energy deviation** over the initial electron phases vanishes, i.e., $<\eta_1>_{\varphi 0} = 0$. Thus, there is no energy exchange between the particles and field at this order. There is, however, energy modulation,

$$\epsilon\eta_1(z) = -\frac{eE_0K[\mathrm{JJ}]k_u L_u^2}{\gamma_r^2 mc^2}\frac{\cos(2k_u\eta_0 z + \phi_0) - \cos\phi_0}{4k_u^2 L_u^2\eta_0}$$
$$\approx -\frac{eE_0K[\mathrm{JJ}]}{2\gamma_r^2 mc^2}\frac{\sin(\ k_u\eta_0 z)\sin(\phi_0)}{2k_u\eta_0} \approx -\frac{eE_0K[\mathrm{JJ}]}{2\gamma_r^2 mc^2} z\sin\phi_0$$

Low-gain regime

Up to now, we view the modulation in η as a precursor to FEL gain, however a variety of longitudinal phase space manipulation techniques take advantage of this phenomenon by employing an optical laser as the driving EM field.

The FEL gain appears at second order in ε when the energy modulation evolves into a density modulation that can radiate coherently. First, we solve for θ_1

$$\frac{d\theta_1}{dz} = \frac{\cos\theta_0(z) - \cos\phi_0}{2k_u L_u^2 \eta_0}$$

$$\Rightarrow \quad \theta_1(z) = \frac{\sin\theta_0(z) - \sin\phi_0}{(2k_u L_u \eta_0)^2} - \frac{z\cos\phi_0}{2k_u L_u^2 \eta_o}.$$

Thus, the second-order energy equation is

$$\frac{d\eta_2}{dz} = -\frac{\theta_1(z)}{2k_u L_u^2}\cos\theta_0(z)$$

$$\Rightarrow \quad \eta_2(L_u) = -\int_0^{L_u} dz \left[\frac{\cos\theta_0(\sin\theta_0 - \sin\phi_0)}{(2k_u L_u^2)(2k_u L_u \eta_0)^2} - \frac{z\cos\theta_0\cos\phi_0}{(2k_u L_u^3)(2k_u L_u \eta_0)}\right]$$

Low-gain regime

Recall that, $\theta_0(z) = 2k_u\eta_0 z + \phi_0,$

Taking the average over initial phases ϕ_0 yields

$$\langle\cos\theta_0 \sin\theta_0\rangle_{\phi_0} = \frac{1}{2}\langle\sin 2\theta_0\rangle_{\phi_0} = 0,$$

$$\begin{aligned}\langle\cos\theta_0 \sin\phi_0\rangle_{\phi_0} &= \Big\langle\Big[\cos(2k_u\eta_0 z)\cos\phi_0 - \sin(2k_u\eta_0 z)\sin\phi_0\Big]\sin\phi_0\Big\rangle_{\phi_0} \\ &= \frac{1}{2}\sin(2k_u\eta_0 z),\end{aligned}$$

$$\langle\cos\theta_0 \cos\phi_0\rangle_{\phi_0} = \frac{1}{2}\cos(2k_u\eta_0 z)\,.$$

Hence,

$$\langle\eta_2(L_u)\rangle_{\phi_0} = -\frac{1}{2k_u L_u^2}\int_0^{L_u} dz\left[\frac{\sin(2k_u\eta_0 z)}{(2k_u L_u\eta_0)^2} - \frac{z\cos(2k_u\eta_0 z)}{L_u(2k_u L_u\eta_0)}\right].$$

Low-gain regime: gain function

Writing the scaled initial electron deviation from resonance as $x = k_u \eta_0 L_u$, it is straightforward to obtain

$$\langle \eta_2(L_u) \rangle_{\phi_0} = \frac{2x \sin x \cos x - 2 \sin^2 x}{8 k_u L_u x^3} = \frac{1}{16 k_u L_u} \frac{d}{dx} \left(\frac{\sin x}{x} \right)^2 . \tag{3.37}$$

Therefore, the average net change in the electron beam energy at second order is given by

Madey's theorem

$$\langle \Delta \eta \rangle = \langle \epsilon^2 \eta_2(L_u) \rangle = - \frac{e^2 E_0^2 K^2 [\mathrm{JJ}]^2}{4 \gamma_r^4 (mc^2)^2} \frac{k_u L_u^3}{4} g(x), \tag{3.38}$$

where we have introduced the normalized gain function

$$g(x) = - \frac{d}{dx} \left(\frac{\sin x}{x} \right)^2 . \tag{3.39}$$

Low-gain regime: FEL gain

$$g(x) = -\frac{d}{dx}\left(\frac{\sin x}{x}\right)^2$$

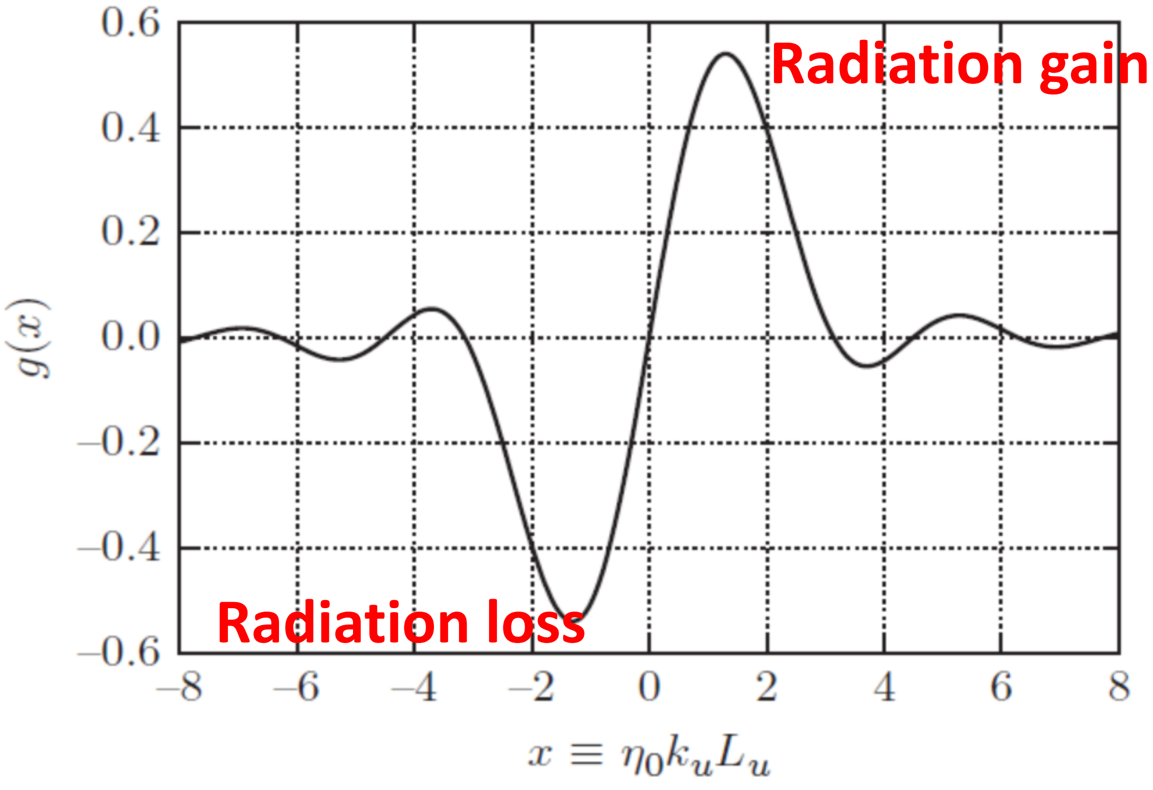

FEL Gain maximum：

x=1.3, g(x)=0.54

And the optimal initial energy offset:

$$\left.\frac{\gamma_0 - \gamma_r}{\gamma_r}\right|_{\substack{\text{max}\\\text{gain}}} = \frac{1.3}{2\pi N_u} \approx \frac{1}{5N_u}$$

The rms width of the gain curve is of order unity around its maximum, which translates to a deviation in beam energy:

$$\Delta\eta \sim 1/6N_u.$$

Using the resonance condition, the frequency width of the gain curve is

$$\frac{\sigma_\omega}{\omega_r} \sim 2\Delta\eta \sim \frac{1}{3N_u}.$$

Low-gain regime: Saturation

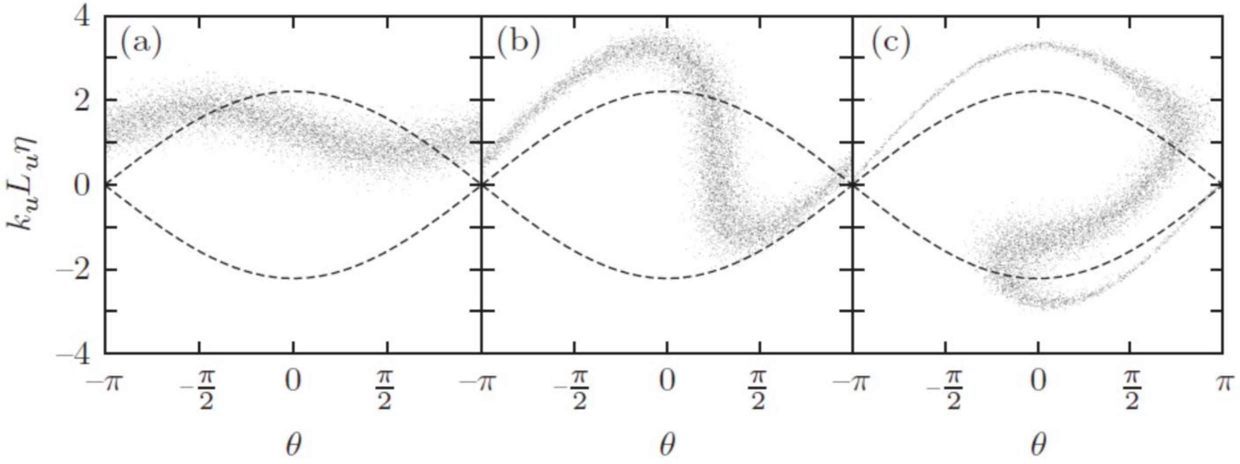

Numerical illustrations of longitudinal phase space at the beginning (a), middle (b), and end (c) of the undulator for a saturated FEL oscillator. The dashed lines show the separatrix of the bucket, while the beam is initially centered at the optimal energy for gain defined by $k_u L_u \eta \approx 1.3$

Maximum energy exchange will occur at particle motion from the top to bottom of the phase space:

$$\Omega_s L_u = \sqrt{\epsilon} \approx \pi$$

The electron contribution to the optical energy:

$$mc^2 \gamma \eta_{\max} = mc^2 \gamma \frac{\sqrt{\epsilon}}{k_u L_u} = mc^2 \gamma \frac{1}{2N_u},$$

The efficiency of an FEL oscillator：

$$\eta_{max} \approx \frac{1}{2N_u}$$

The ideal output power for FEL oscillator can be estimated:

$$\Delta P \approx \frac{1}{2N_u} P_{beam}$$

Note of FELO: low-gain saturation ⟺ *cavity saturation*

High gain FEL theory

High-gain regime

High Gain FEL – Exponential Growth

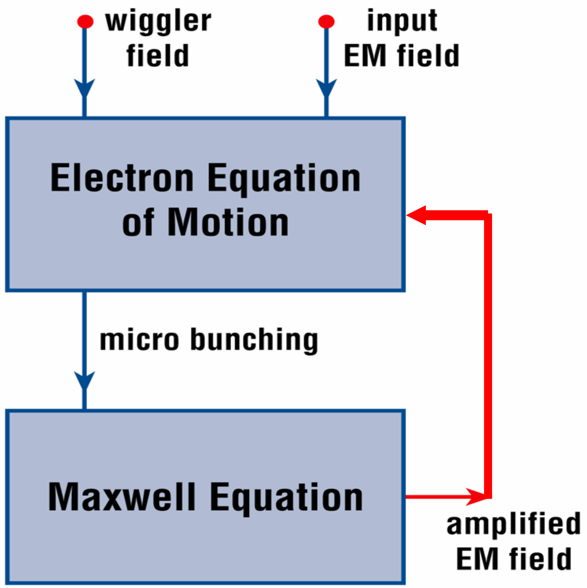

1D Theory: exponential growth, proposes SASE (Self Amplified Spoontaneous Emission)

Saldin *et.al.* (1982)
Bonifacco, Pellegini *et. al* (1984)

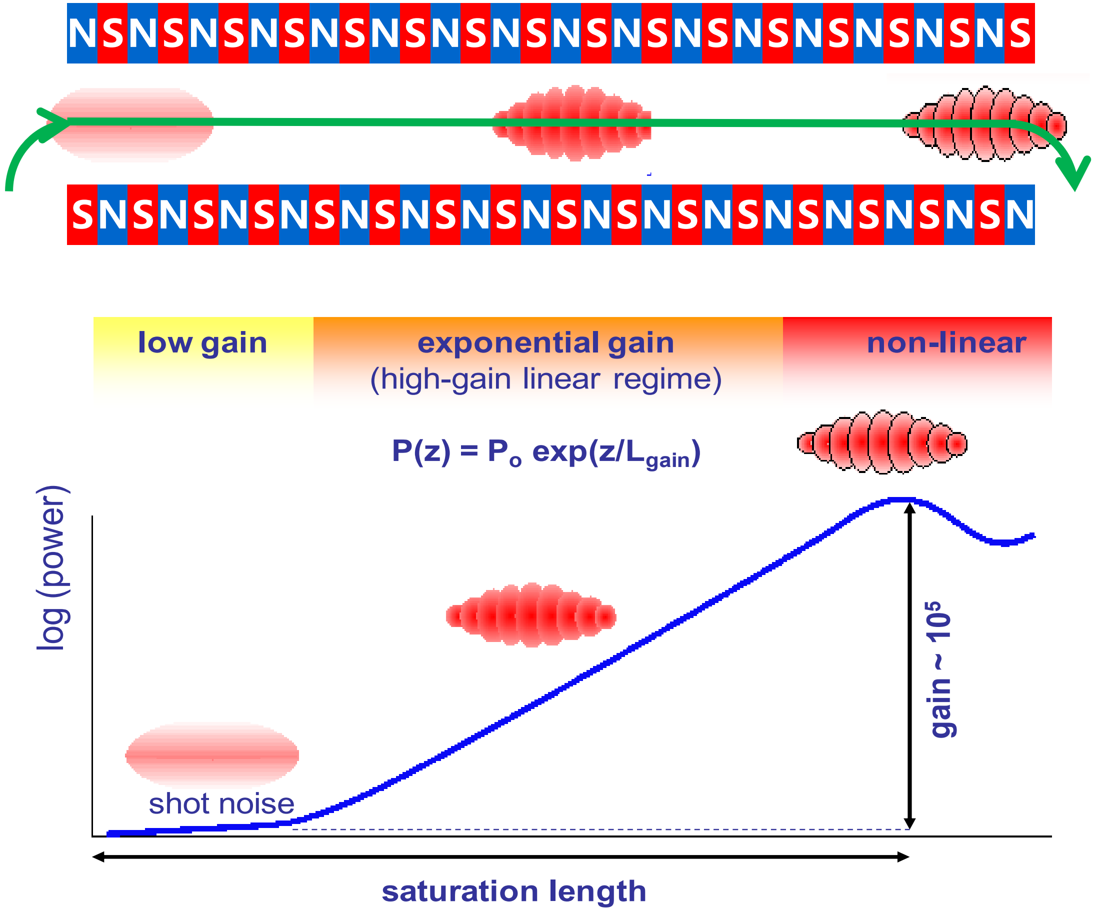

1D Maxwell Equation

- 1D Maxwell equation for the transverse electric field

$$\left[\left(\frac{1}{c}\frac{\partial}{\partial t}\right)^2 - \left(\frac{\partial}{\partial z}\right)^2 - \nabla_\perp^2\right] E_x = -\frac{1}{\varepsilon_0 c^2}\left[\frac{\partial J_x}{\partial t} + c^2 \frac{\partial \rho_e}{\partial x}\right]$$

- Transverse current density

$$J_x = -\frac{ecK}{2\pi\sigma_x^2}\cos(k_u z)\sum_{j=1}^{N_e}\frac{1}{\gamma_j}\delta[z - z_j(t)],$$

- Use slowly varying phase and amplitude approximation

$$E_x(z,t) = \tilde{E}(z,t)\cos[k_1 z - \omega_1 t + \phi(z,t)]. \quad \Rightarrow \quad E_x = E(z,t)e^{i(k_1 z - \omega_1 t)} + E^*(z,t)e^{-i(k_1 z - \omega_1 t)}.$$

- Final Maxwell equation

$$\tilde{E}(z,t) = Ee^{i\phi}/2$$

$$\left[\frac{\partial}{\partial z} + \frac{1}{c}\frac{\partial}{\partial t}\right] E = -\chi_2 n_e \langle e^{-i\theta_j}\rangle_\Delta \qquad \chi_2 = \frac{eK[\mathrm{JJ}]}{4\epsilon_0\gamma_r}$$

FEL equations

- Change the field equation variables from (t , z) to (θ, z)

Using $\theta = (k_1 + k_u)z - ck_1 t$, we have

$$\left.\frac{\partial}{\partial z}\right|_t + \frac{1}{c}\left.\frac{\partial}{\partial t}\right|_z = \left.\frac{\partial}{\partial z}\right|_\theta + k_u \left.\frac{\partial}{\partial \theta}\right|_z ,$$

- We obtain

$$\left[\frac{\partial}{\partial z} + k_u \frac{\partial}{\partial \theta}\right] E(\theta; z) = -\chi_2 n_e \langle e^{-i\theta_j} \rangle_\Delta \qquad \chi_2 = \frac{eK[\mathrm{JJ}]}{4\epsilon_0 \gamma_r}$$

- And rewrite the pendulum equations in terms of the slowly varying E

$$\frac{d\theta_j}{dz} = 2k_u \eta,$$
$$\frac{d\eta_j}{dz} = \chi_1 \left(E e^{i\theta_j} + E^* e^{-i\theta_j}\right) \qquad \chi_1 = \frac{eK[\mathrm{JJ}]}{2\gamma_r^2 mc^2}$$

Dimensionless FEL equations

① We introduce the as yet unspecified parameter ρ by defining the scaled longitudinal coordinate $\hat{z} \equiv 2k_u\rho z$ that leads to the phase equation

$$\frac{d\theta_j}{d\hat{z}} = \hat{\eta}_j \quad \text{for} \quad \hat{\eta}_j \equiv \frac{\eta_j}{\rho} \quad \text{(the new “momentum” variable).}$$

② To simplify the energy equation for $\hat{\eta}_j$, we define the dimensionless complex field amplitude

$$a = \frac{\chi_1}{2k_u\rho^2}E,$$

in terms of which the energy equation reduces to

$$\frac{d\hat{\eta}_j}{d\hat{z}} = a(\theta_j, \hat{z})e^{i\theta_j} + a(\theta_j, \hat{z})^* e^{-i\theta_j}.$$

③ Writing the field equation in terms of $\hat{z}$ and a, we have

$$\left[\frac{\partial}{\partial \hat{z}} + \frac{1}{2\rho}\frac{\partial}{\partial \theta}\right] a(\theta, \hat{z}) = -\frac{\chi_1}{2k_u\rho^2}\frac{n_e\chi_2}{2k_u\rho}\langle e^{-i\theta_j}\rangle_\Delta.$$

Set it to 1

FEL Pierce parameter ρ

- To simplify the field equation, set the coefficient on its right-hand-side to unity. Thus, the dimensionless FEL pierce parameter must be

$$\rho = \left[\frac{n_e \chi_1 \chi_2}{(2k_u)^2}\right]^{1/3} = \left(\frac{e^2 K^2 [\mathrm{JJ}]^2 n_e}{32 \epsilon_0 \gamma_r^3 m c^2 k_u^2}\right)^{1/3} = \left[\frac{1}{8\pi}\frac{I}{I_A}\left(\frac{K[\mathrm{JJ}]}{1+K^2/2}\right)^2 \frac{\gamma \lambda_1^2}{2\pi\sigma_x^2}\right]^{1/3}$$

; I_A=17 kA is Alfven current

- At saturation, electrons are fully bunched so that $|\langle e^{-i\theta_j}\rangle_\Delta| \rightarrow 1$, which implies maximum radiation amplitude |a|→1, and translate it to $|E| \rightarrow 2k_u\rho^2/\chi_1$, so that the maximum field energy density

$$2\epsilon_0 |E|^2 \sim 2\epsilon_0 \rho \frac{4k_u^2 \rho^3}{\chi_1^2} = 2\epsilon_0 \rho \frac{\chi_2}{\chi_1} = \rho n_e \gamma_r m c^2.$$

- Because $n_e m c^2 \gamma_r$ is the electron energy density, we see that $\boldsymbol{\rho}$ presents the FEL efficiency at saturation, and FEL saturation power ~ ρ×(e-beam power)

$$\rho = \frac{\text{field energy generated}}{\text{e-beam kinetic energy}}.$$

1D solution

- Illustrate the essentials of FEL gain by neglecting the θ dependence of the electromagnetic field. The 1D FEL equation are

$$\frac{d\theta_j}{d\hat{z}} = \hat{\eta}_j$$

$$\frac{d\hat{\eta}_j}{d\hat{z}} = ae^{i\theta_j} + a^* e^{-i\theta_j}$$

$$\frac{da}{d\hat{z}} = -\langle e^{-i\theta_j} \rangle_\Delta \,.$$

$$\boxed{\hat{z} = 2\rho k_u z}$$

$$\boxed{\hat{\eta} = \frac{\eta}{\rho}}$$

These are $2N_\Delta + 2$ coupled first order ordinary differential equations, $2N_\Delta$ for the particles, and 2 equations for the complex amplitude a. In general, these can only be solved via computer simulation.

Three coupled first-order equations

- However, the system can be linearized in terms of three collective variables

$$a \qquad \text{(field amplitude)}$$

$$b = \langle e^{-i\theta_j} \rangle_\Delta \qquad \text{(bunching parameter)}$$

$$P = \langle \hat{\eta}_j e^{-i\theta_j} \rangle_\Delta \qquad \text{(collective momentum).}$$

Three coupled first-order equations:

$$\frac{da}{d\hat{z}} = -b \qquad \text{Bunching produces coherent radiation.}$$

$$\frac{db}{d\hat{z}} = -iP \qquad \text{Energy modulation becomes density bunching.}$$

$$\frac{dP}{d\hat{z}} = a \qquad \text{Coherent radiation drives energy modulation.}$$

Cubic equation

These are three coupled first order equations, which can be reduced to a single third-order equation for a as

$$\frac{d^3 a}{d\hat{z}^3} = ia.$$

We solve the linear equation by assuming that the field dependence is $\sim e^{-i\mu\hat{z}}$, which results in the following dispersion relation for μ:

$$\mu^3 = 1.$$

This is the well-known cubic equation [14], whose three roots are given by

$$\mu_1 = 1, \qquad \mu_2 = \frac{-1-\sqrt{3}i}{2}, \qquad \mu_3 = \frac{-1+\sqrt{3}i}{2}.$$

The root μ_1 is real and gives rise to an oscillatory solution, while μ_2 and μ_3 are complex conjugates that lead to exponentially decaying and growing modes, respectively.

Exponential solution

- General solution: $a(\hat{z}) = \sum_{\ell=1}^{3} C_\ell e^{-i\mu_\ell \hat{z}}.$
- Solving based on the initial conditions: $a(\hat{z}) = \frac{1}{3}\sum_{\ell=1}^{3}\left[a(0) - i\frac{b(0)}{\mu_\ell} - i\mu_\ell P(0)\right] e^{-i\mu_\ell \hat{z}}.$
- At a short distance, the growing, decaying and oscillating modes compete with one another.
- At a long distance, the exponentially growing mode dominates

$$a(\hat{z}) \approx \frac{1}{3}\left[a(0) - i\frac{b(0)}{\mu_3} - i\mu_3 P(0)\right] e^{-i\mu_3 \hat{z}}.$$

Seeded SASE(bunched) Energy-modulation (Pre-bunched)

- Consider the case of SASE (no seed and no energy modulation)

$$\langle |a(\hat{z})|^2 \rangle \approx \frac{1}{9}\langle |b(0)|^2 \rangle e^{\sqrt{3}\hat{z}}.$$

Here, the scaled propagation distance $\sqrt{3}\hat{z} = \sqrt{3}(2k_u z\rho) = z/L_{G0}$, and the ideal 1D power gain length is $L_{G0} \equiv \frac{\lambda_u}{4\pi\sqrt{3}\rho}.$

High-gain FEL Analysis

Gain function

- Considering an energy deviation η:

$$\tilde{E}_x(\eta, z) = \sum_{j=1}^{3} c_j(\eta) \exp(\alpha_j(\eta) z)$$

- Gain function:

$$G(\eta, z) = \left| \frac{\tilde{E}_x(\eta, z)}{E_{\text{in}}} \right|^2 - 1$$

- Within the first two gain length, gun function agrees with low gain FEL theory.
- In a long undulator, power growth, energy deviation and gain bandwidth are different.

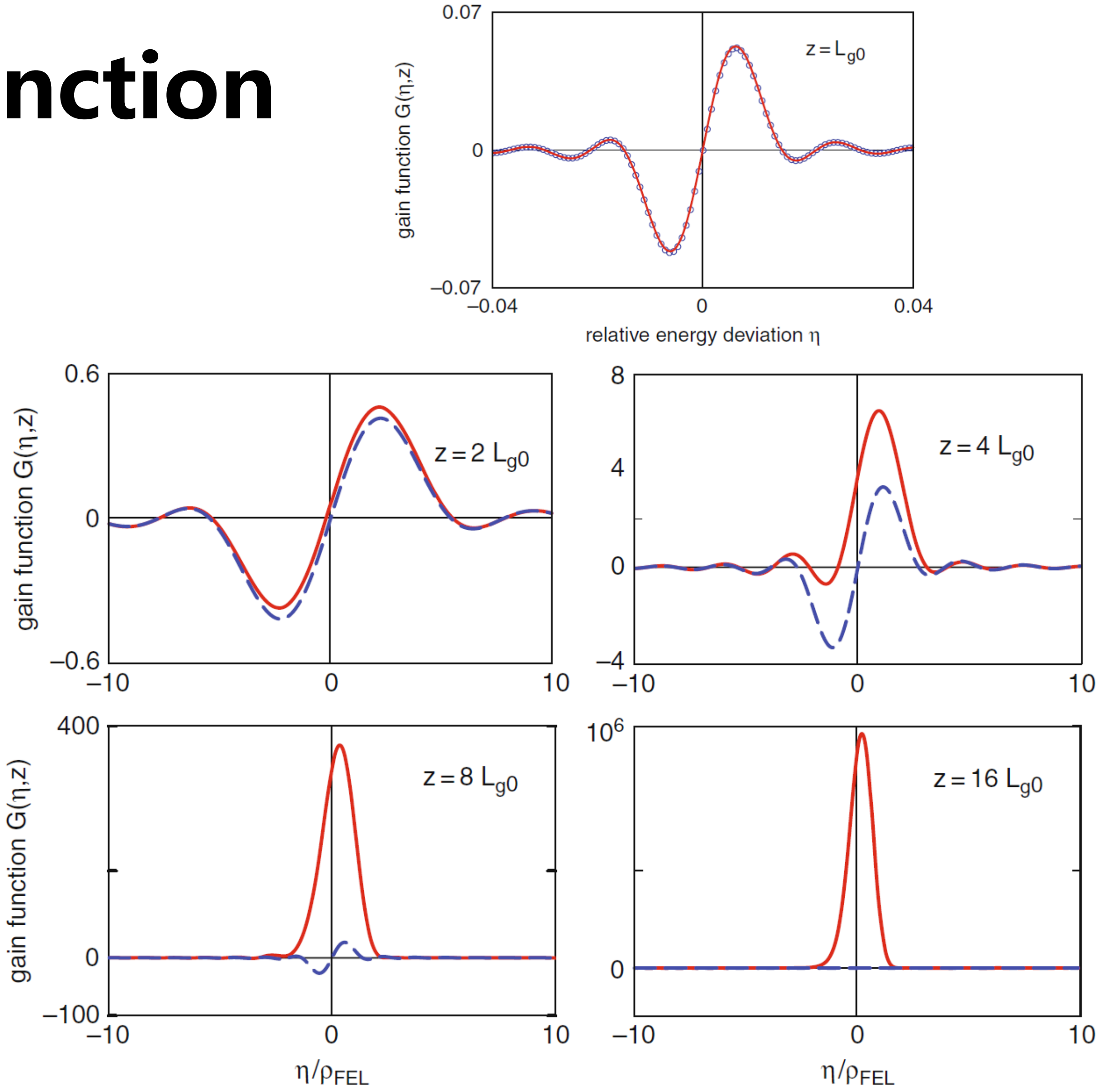

Red curve: high gain; blue curve: low gain

FEL bandwidth

- FEL bandwidth is dominated by the FEL Pierce parameter ρ
- Considering an energy deviation η, the eigenvalue of the exponential gain term can be expanded in a Taylor series

$$\Re\{\alpha_1(\eta)\} \approx \frac{1}{2L_{g0}}\left(1-\frac{\eta^2}{9\,\rho_{FEL}^2}\right) .$$

From this follows that the gain curve in the exponential regime can be approximated by a Gaussian[1]

$$G(\eta,z) \propto \exp(z/L_{g0})\ \exp\left(-\frac{\eta^2 z}{9\,\rho_{FEL}^2 L_{g0}}\right) = \exp(z/L_{g0})\ \exp\left(-\frac{\eta^2}{2\tau^2}\right)$$

with a z dependent variance

$$\tau^2 = \frac{9\,\rho_{FEL}^2 L_{g0}}{2z} . \qquad \eta = \eta(\omega) = -\frac{\omega-\omega_r}{2\omega_r} \quad \text{with} \quad \omega_r = \frac{2\gamma_r^2 c\,k_u}{1+K^2/2} .$$

From (5.7) follows that the rms frequency bandwidth of a SASE FEL is

$$\boxed{\sigma_\omega(z) = \tau(z)\,2\,\omega_\ell = 3\sqrt{2}\,\rho_{FEL}\,\omega_\ell\sqrt{\frac{L_{g0}}{z}} .}$$

Only valid in the high gain regime.

High gain FEL saturation

- The exponential growth cannot continue indefinitely because the beam energy decreases due to the energy loss by radiation and the modulated current density $\tilde{j}_1$ becomes eventually comparable in magnitude to the DC current density j_0.
- We assume full modulation, i.e. $|\tilde{j}_1| = |j_0|$ The major part of the intensity is generated in the last section of the exponential regime. The field amplitude at saturation is approximately given by the slope of the field gain curve, multiplied with the field gain length.

$$\left|\tilde{E}_x\right|_{\mathrm{sat}} \approx \left|\frac{d\tilde{E}_x}{dz}\right| \cdot 2\,L_{\mathrm{g0}} = \frac{\mu_0 c\,\widehat{K}}{4\gamma_r}\,|j_0|\,2\,L_{\mathrm{g0}}$$

- The saturation power is:

$$P_{\mathrm{sat}} = \frac{c\varepsilon_0}{2}\left|\tilde{E}_x\right|^2_{\mathrm{sat}} A_b \approx \frac{c\varepsilon_0}{2}\left(\frac{\mu_0 c\,\widehat{K}}{4\gamma_r}\right)^2 \frac{I_0^2}{A_b}\,4\,L_{\mathrm{g0}}^2$$

- The electron beam power is $P_{beam} = \gamma_s m_e c^2 I_0/e = E_0\, I_0$, and one can estimates the FEL power at saturation

$$P_{\mathrm{sat}} \approx \rho_{\mathrm{FEL}}\, P_{\mathrm{beam}}$$

中國科學院上海高等研究院
SHANGHAI ADVANCED RESEARCH INSTITUTE, CHINESE ACADEMY OF SCIENCES

FEL gain curve

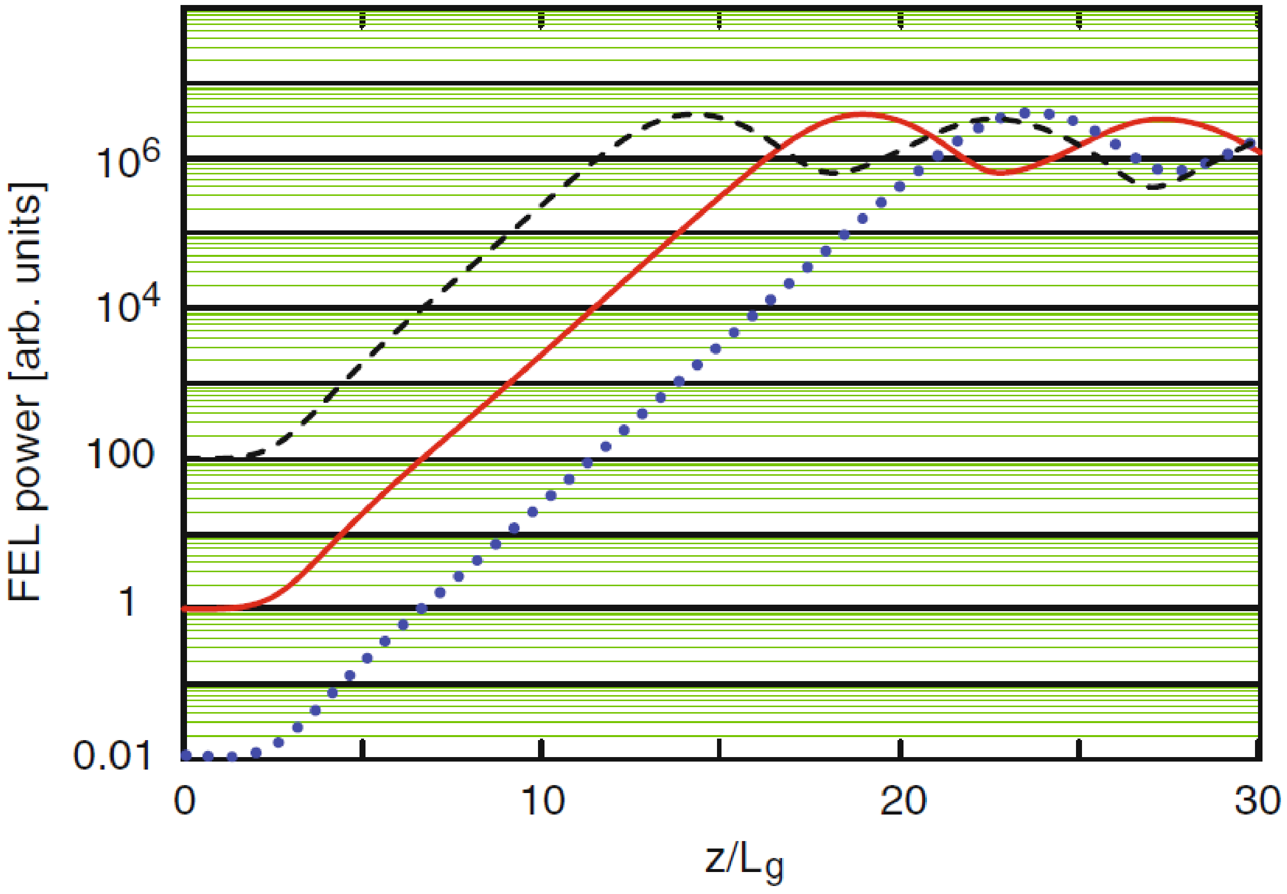

Phase space evolution

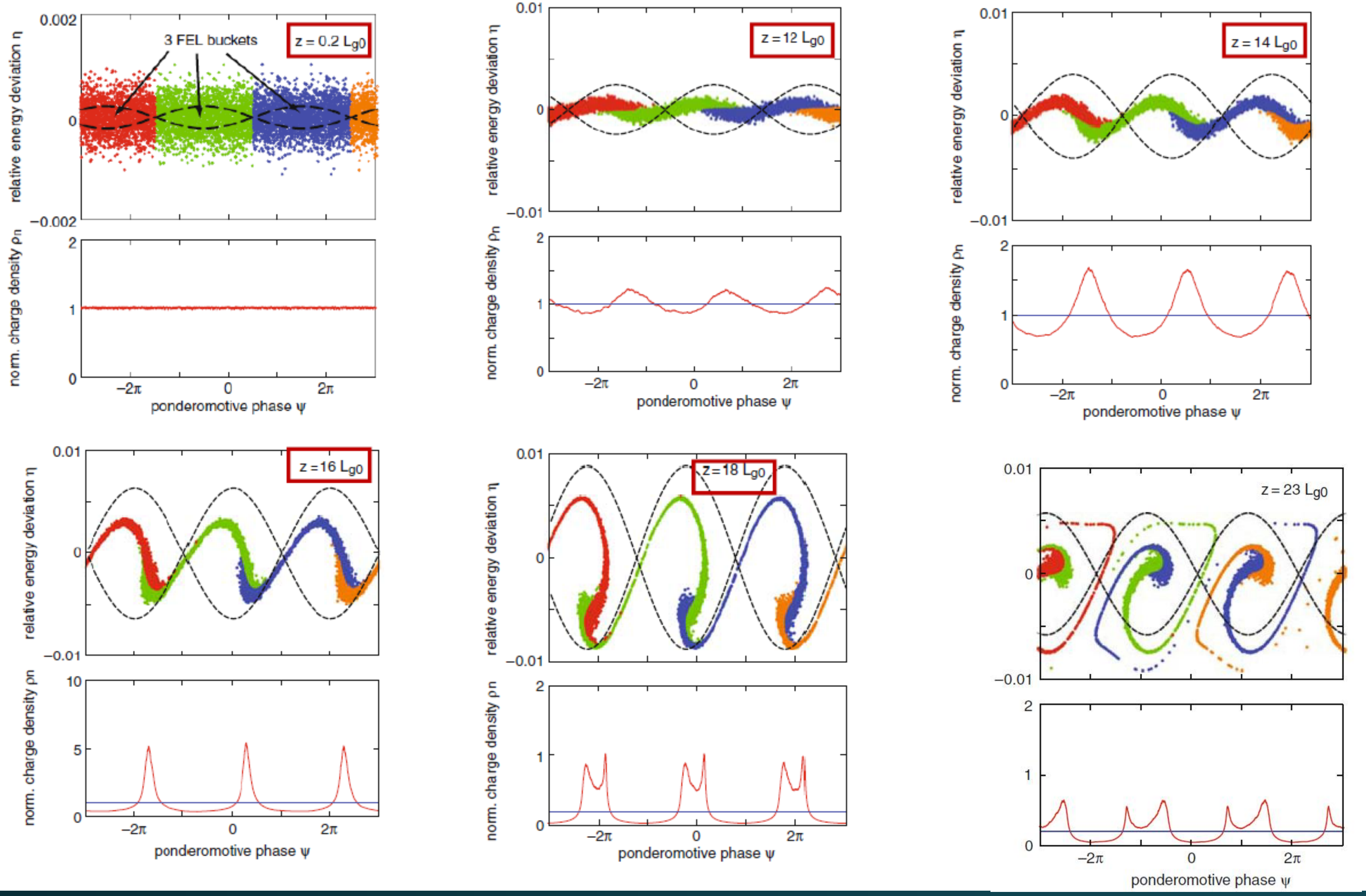

$$\eta_{\rm sep}(\psi) = \pm\sqrt{\frac{e\left|\tilde{E}_x(z)\right|\widehat{K}}{k_u m_e c^2 \gamma_r^2}}\cos\left(\frac{\psi - \psi_b(z)}{2}\right)$$

Self-Amplified Spontaneous Emission (SASE)

What is SASE ?

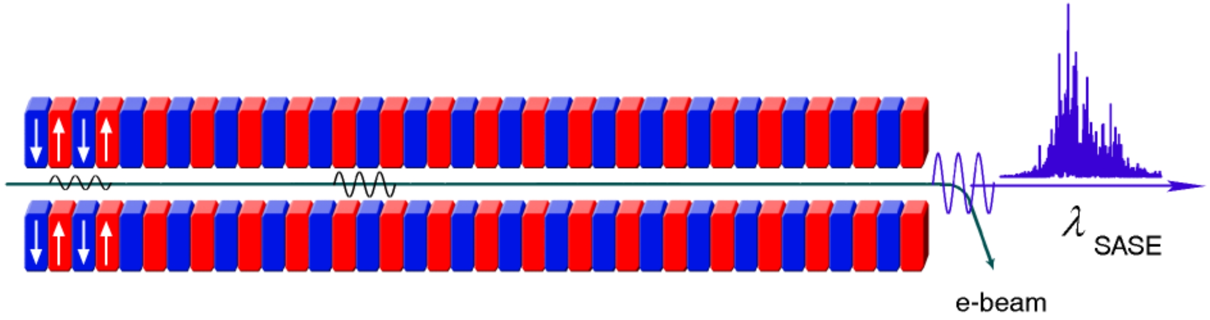

- **SASE was proposed in 1980s and experimentally demonstrated at DESY TTF in 2001 at 109nm.**
- **SASE-based hard x-ray FEL facilities all over the world.**
- **SASE eliminates an optical cavity and starts from shot noise, resulting in the lack of longitudinal coherence.**

electron arrival time t is random

➔ spontaneous emission

➔ amplified by FEL interaction

➔ quasi-coherent x-rays

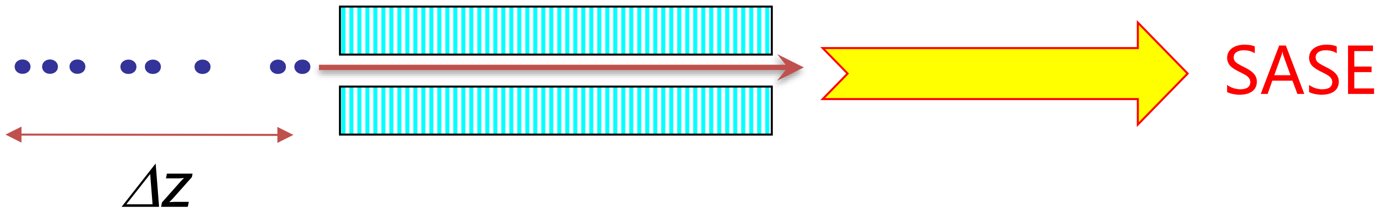

Qualitative description

- In the high gain regime, we use the radiation intensity in the exponential growth regime

$$\langle |a(\hat{z})|^2 \rangle \approx \frac{1}{9} \langle |b(0)|^2 \rangle e^{\sqrt{3}\hat{z}}$$

- The bunching factor at the undulator entrance b(0) derives from the initial shot noise of the beam, which is subsequently amplified by the FEL process. This input noise turns out to be approximately given by the spontaneous undulator radiation generated in the first gain length of the undulator.

$$\langle |b(0)|^2 \rangle = \left\langle \frac{1}{N_{l_{\mathrm{coh}}}^2} \left| \sum_{j \in l_{\mathrm{coh}}} e^{-i\theta_j} \right|^2 \right\rangle \approx \frac{1}{N_{l_{\mathrm{coh}}}},$$

Electrons number in a coherence length

- Slippage leads to coherence length as well as spiky structure. Coherence length is usually constructed as slippage over 2 gain length and increases depending on the z position in the undulator

$$\tau_{\mathrm{coh}} \approx \frac{\sqrt{\pi}}{\sigma_\omega} \qquad \sigma_\omega = \sigma_\omega(z) = 3\sqrt{2}\,\rho_{\mathrm{FEL}}\,\omega_\ell \sqrt{\frac{L_{\mathrm{g0}}}{z}} \quad \Rightarrow \quad l_{\mathrm{coh}} \sim \lambda_1/\rho$$

Statistical fluctuation

- Due to noise start-up, SASE is a chaotic light temporally with M_L coherent modes (M_L spikes in intensity profile)

$$M_L \approx \frac{\text{bunch length}}{\text{coherence length}} = \frac{T_b}{\tau_{\text{coh}}}$$

- Usually bunch length is much larger than the coherence length, and the longitudinal phase space is M_L larger than FT limit.
- Integrated energy fluctuation $\dfrac{\Delta W}{W} = \dfrac{1}{\sqrt{M_L}}$
- Singe spike intensity fluctuates 100%
- M_L is NOT a constant, decreases due to increasing coherence in the exponential growth, and increases due to decreasing coherence after saturation.

Typical SASE spectrum

- Spectral properties are similar to temporal domain, except that everything is inverted

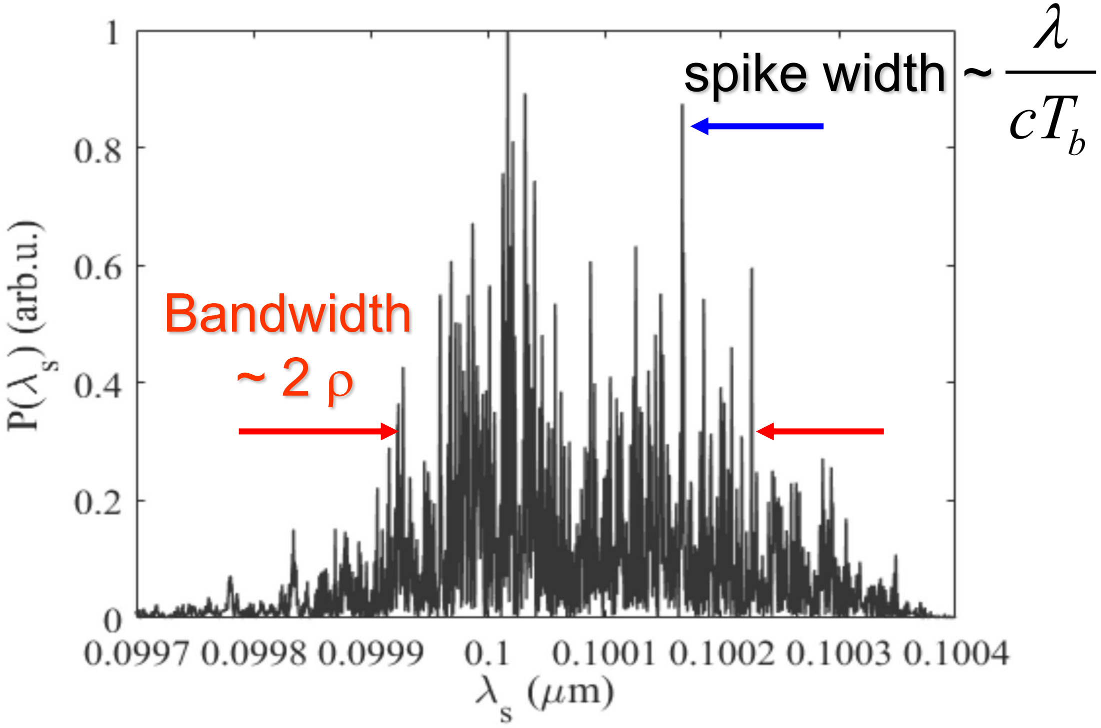

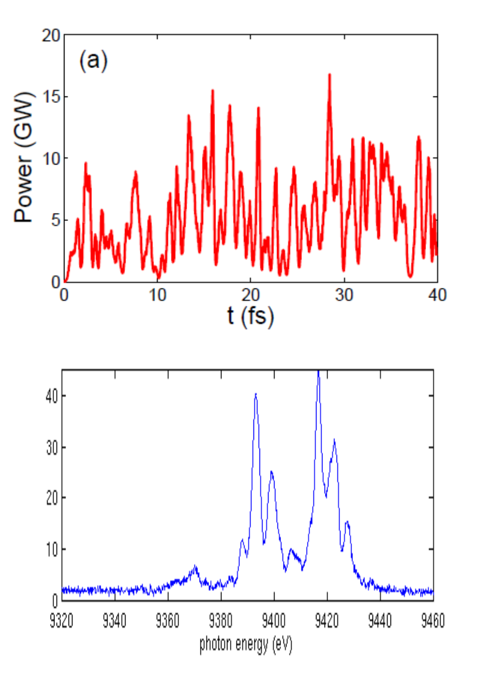

Bunch length	⟺	**Spike bandwidth**
Coherence length	⟺	**SASE bandwidth**

FEL startup from e-beam noise

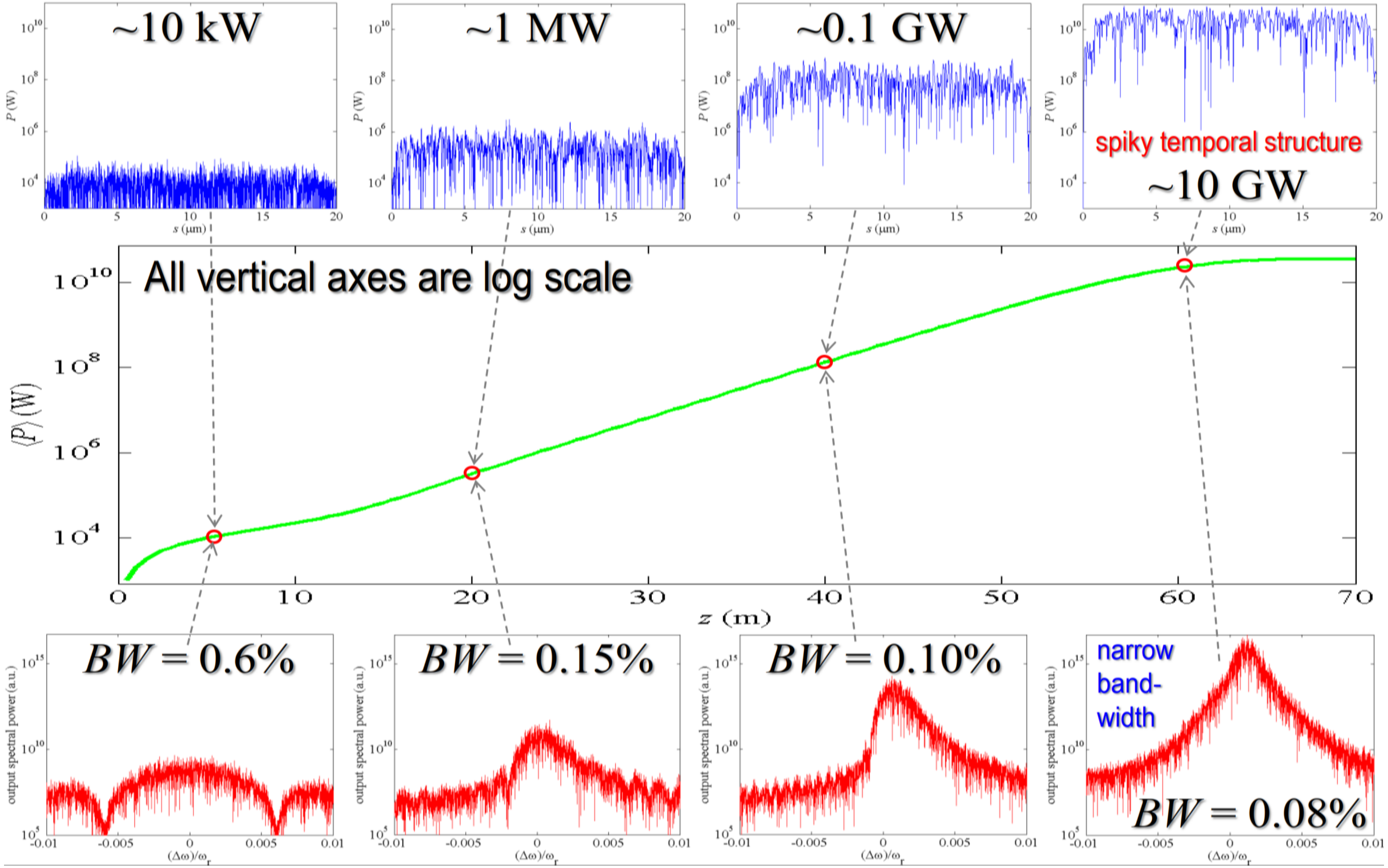

Transverse coherence

Z=25m

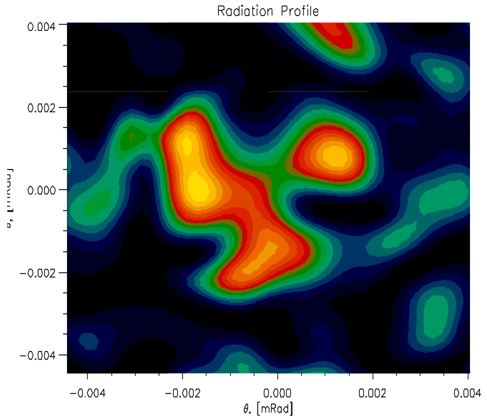

Z=37.5m

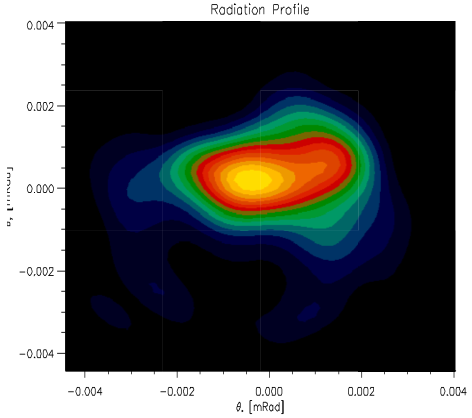

Z=50m

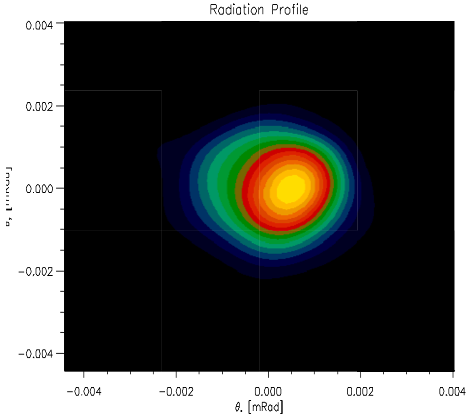

Z=62.5m

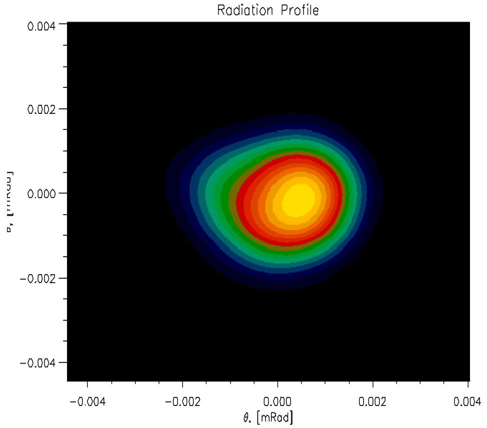

Z=75m

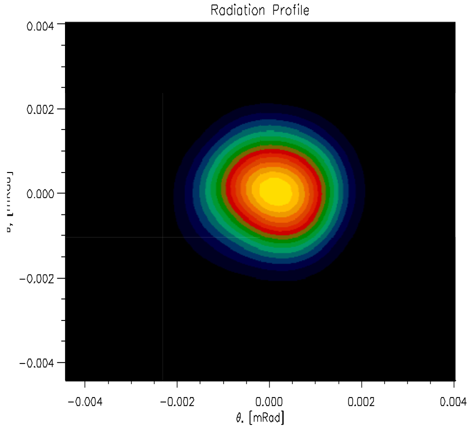

Z=87.5m

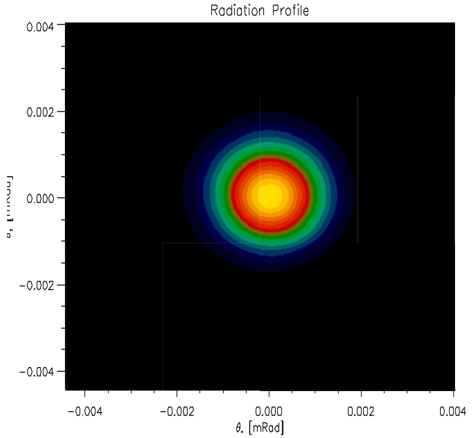

Single mode dominates ➔ close to 100% transverse coherence

SASE 1D Summary

- Power gain length $L_{G0} = \frac{\lambda_u}{4\pi\sqrt{3}\rho}$
- Exponential growth $P = (1/9)P_n \exp(z/L_G)$
- Startup noise power $P_n \sim \rho^2 \gamma mc^3/\lambda_r$
~ spontaneous radiation in two power gain length
- Saturation power ~ ρ x e-beam power
- Saturation length ~ $\lambda_u/\rho \sim 20\ L_G$
- RMS bandwidth at saturation ~ ρ
- Temporal coherence length at saturation ~ λ_r/ρ

Three-dimensional effects

	Ming-Xie parameters	Conditions for 1D Theory
Diffraction $L_{1D} \leq z_R$	$\eta_d = \dfrac{L_{1D}}{z_R}$	$\eta_d < 1$ $z_R > L_{1D}$
Emittance $\dfrac{L_{1D}}{\beta_{ave}} \dfrac{4\pi\varepsilon_u}{\lambda_r} \leq 1$	$\eta_\varepsilon = \dfrac{L_{1D}}{\beta_{ave}} \dfrac{4\pi\varepsilon_u}{\lambda_r}$	$\eta_\varepsilon < 1$ $\beta_{ave} > L_{1D}$
Energy spread $\dfrac{\sigma_\gamma}{\gamma} \leq \dfrac{1}{4\pi N_G}$	$\eta_\gamma = \dfrac{4\pi L_{1D}}{\lambda_u} \dfrac{\sigma_\gamma}{\gamma}$	$\eta_\gamma < 1$ $\dfrac{\sigma_\gamma}{\gamma} < \rho$

Ming-Xie’s 3D fitting formula

3D effects increase the power gain length by a factor $F(\eta_d,\eta_\varepsilon,\eta_\gamma) = 1 + \Lambda(\eta_d,\eta_\varepsilon,\eta_\gamma)$

$$\Lambda(\eta_d,\eta_\varepsilon,\eta_\gamma) = a_1{\eta_d}^{a_2} + a_3{\eta_\varepsilon}^{a_4} + a_5{\eta_\gamma}^{a_6} + a_7{\eta_\varepsilon}^{a_8}{\eta_\gamma}^{a_9} + a_{10}{\eta_d}^{a_{11}}{\eta_\gamma}^{a_{12}} + a_{13}{\eta_d}^{a_{14}}{\eta_\varepsilon}^{a_{15}} + a_{16}{\eta_d}^{a_{17}}{\eta_\varepsilon}^{a_{18}}{\eta_\gamma}^{a_{19}}$$

a_1=0.45	a_2=0.57	a_3=0.55	a_4=1.6
a_5=3	a_6=2	a_7=0.35	a_8=2.9
a_9=2.4	a_{10}=51	a_{11}=0.95	a_{12}=3
a_{13}=5.4	a_{14}=0.7	a_{15}=1.9	a_{16}=1140
a_{17}=2.2	a_{18}=2.9	a_{19}=3.2	

3D Power gain length $L_{G,3D} = L_{g0}(1+\Lambda)$

3D Saturated power $P_{sat,3D} = \dfrac{\rho P_b}{(1+\Lambda)^2}$

Fully coherent FEL

Towards fully coherence

SASE is inherently chaotic and noisy

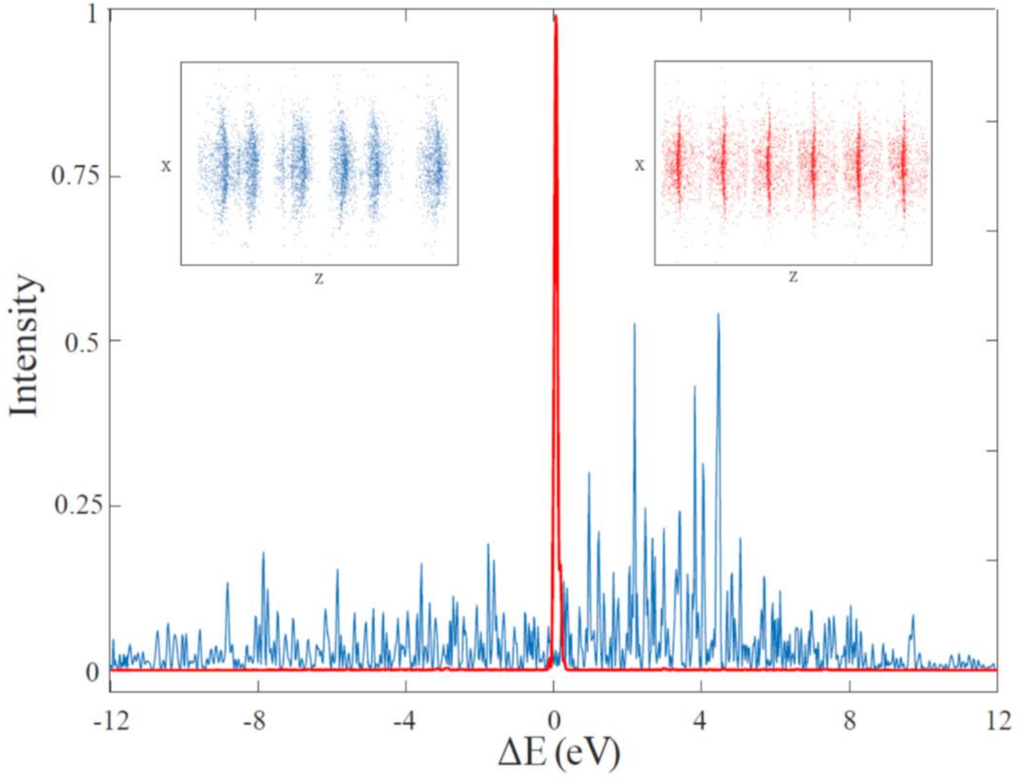

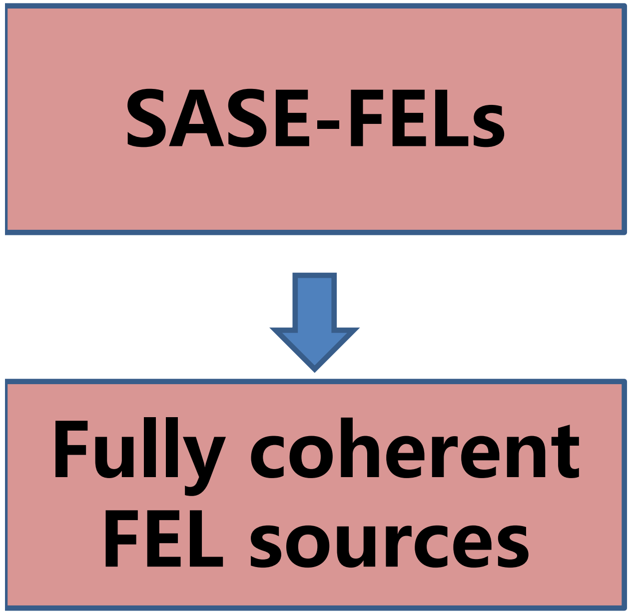

SASE & its advances

- ✓ pSASE (Purified SASE)
- ✓ iSASE (Improved SASE)
- ✓ HB-SASE
- ✓ Mode locked SASE

Seeding schemes

- ✓ HGHG, EEHG, EEHC…
- ✓ SXRSS, HXRSS
- ✓ XFELO

Seedings schemes

With seed laser

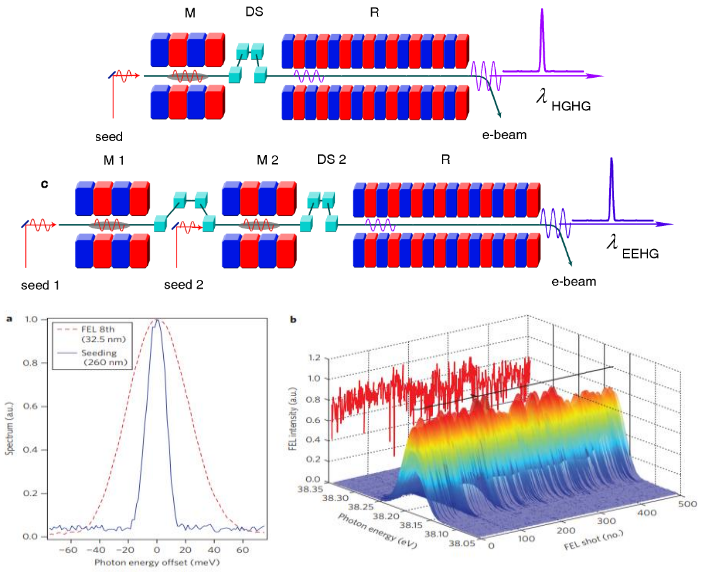

External-seeding

- ✓ **HGHG, EEHG, EEHC…**
- ✓ **FERMI、DCLS、SXFEL、…**
- ✓ **UV to soft X-Ray**
- ✓ **Complex system**

Without seed laser

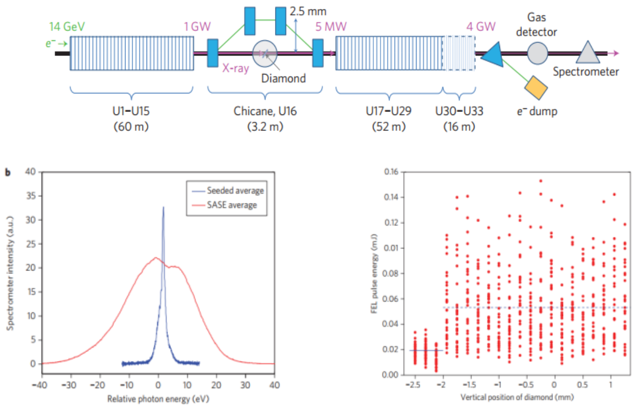

Self-seeding

- ✓ **SXRSS, HXRSS**
- ✓ **LCLS、PAL-XFEL、EXFEL、SACLA、SHINE…**
- ✓ **Soft and Hard X-ray**
- ✓ **Stability limited by SASE**

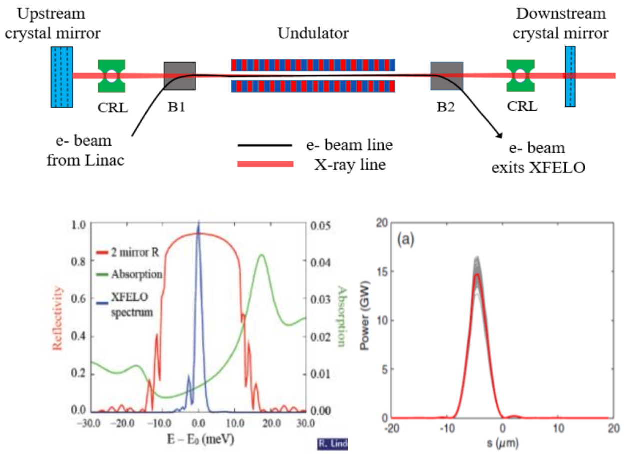

Cavity based X-ray FEL

- ✓ **XFELO (and RAFEL)**
- ✓ **R&D (first demonstrated in May, 2025)**
- ✓ **Simple system and stable output**
- ✓ **Depend on cavity**
- ✓ **Ideal fully coherent hard X-ray**

Self-seeding

Hard and soft x-ray self-seeding

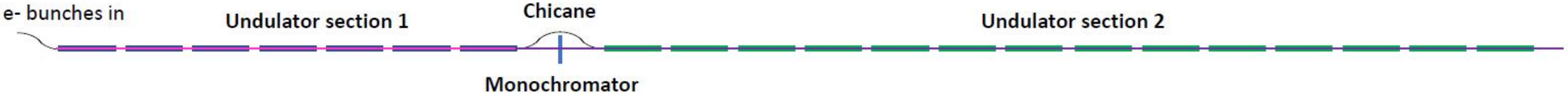

SASE is produced in Undulator Section 1

Coherent seed is amplified in Undulator Section 2

Monochromator filters SASE to produce coherent seed

Hard X-ray Self-Seeding (HXRSS)
Monochromator = thin Bragg crystal

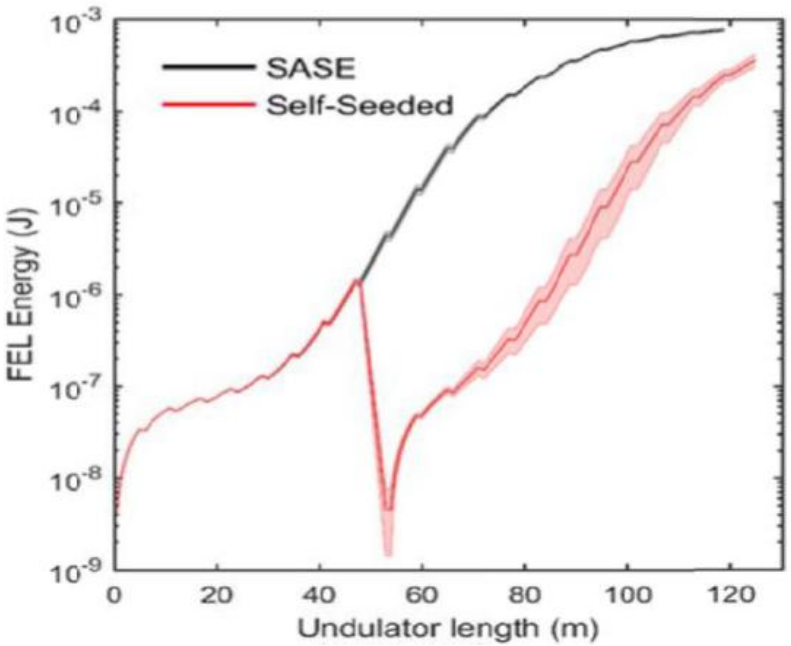

Soft X-ray Self-Seeding
Monochromator = a toroidal grating

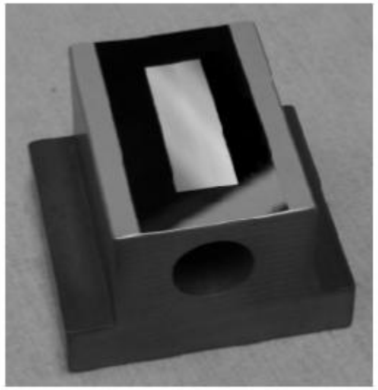

Hard x-ray self-seeding

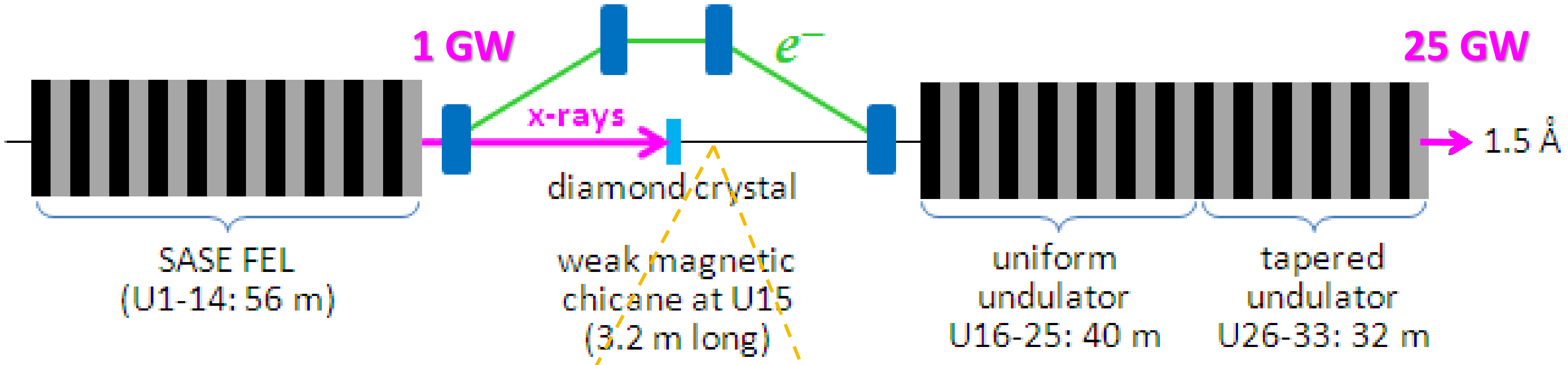

Geloni, Kocharyan, Saldin (*DESY*)

FEL spectrum after diamond

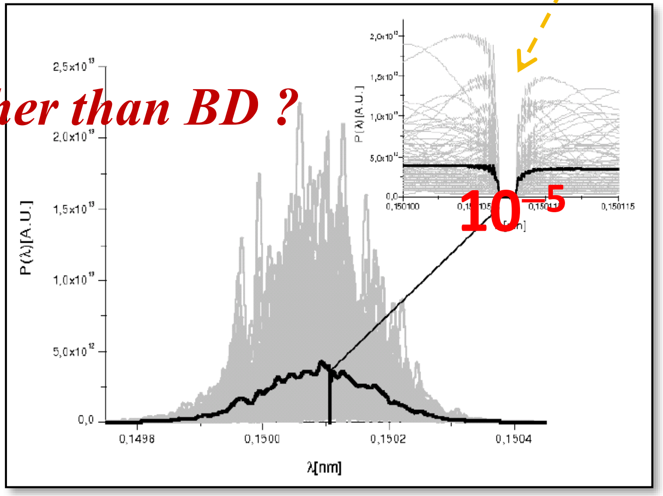

Why is it FBD, other than BD ?

Power dist. after diamond

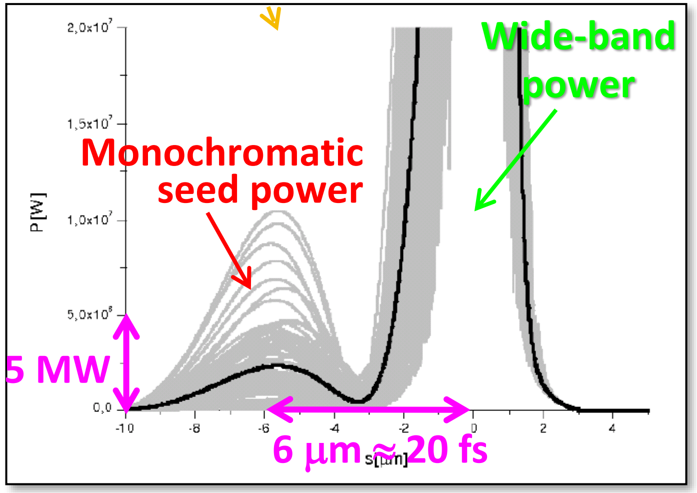

Self-seeding of 1mm electron bunch at 0.15nm yields **10^{-4} BW** with low charge mode

How does HXRSS generate wake pulses

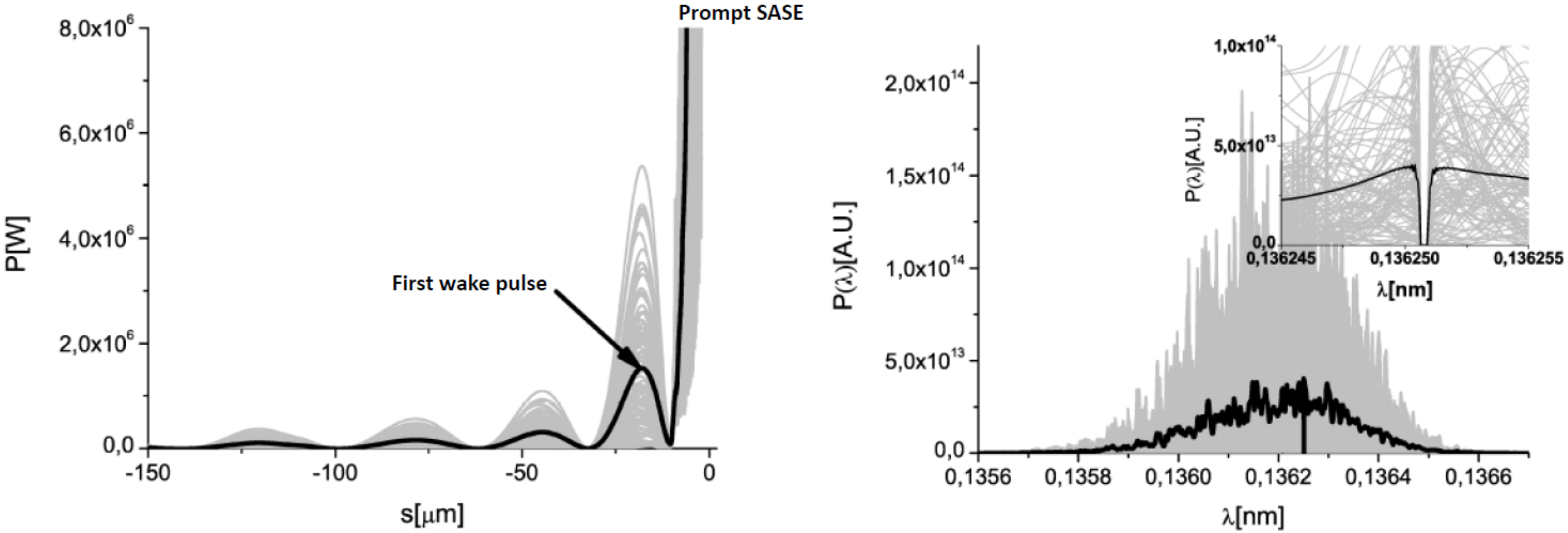

Bragg diffraction creates a spectral "notch" in the SASE spectrum. The Forward Bragg Diffraction (FBD) frequencies adjacent to the "notch" interfere constructively and destructively. In the time domain, this interference produces monochromatic wake pulses that follow the prompt SASE pulse.

L. Geloni et al., J. Mod. Opt. 58, 1391 (2011)

Bragg spectral response function

- Monochromator: BD vs FBD

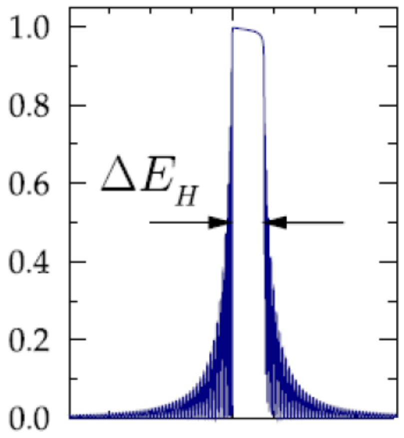

Reflected Bragg spectral response function

$$R_{0H} = R_1 R_2 \frac{1 - e^{i(\chi_1 - \chi_2)d}}{R_2 - R_1 \, e^{i(\chi_1 - \chi_2)d}}$$

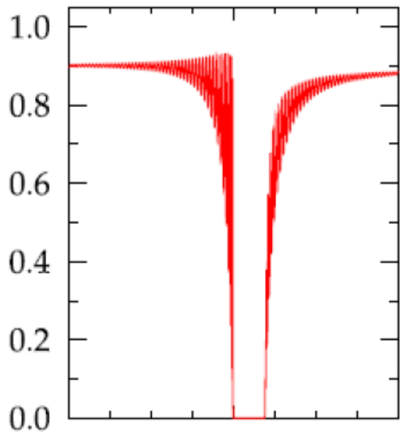

Forward Bragg spectral response function

$$R_{00} = e^{i\chi_1 d} \frac{R_2 - R_1}{R_2 - R_1 \, e^{i(\chi_1 - \chi_2)d}}$$

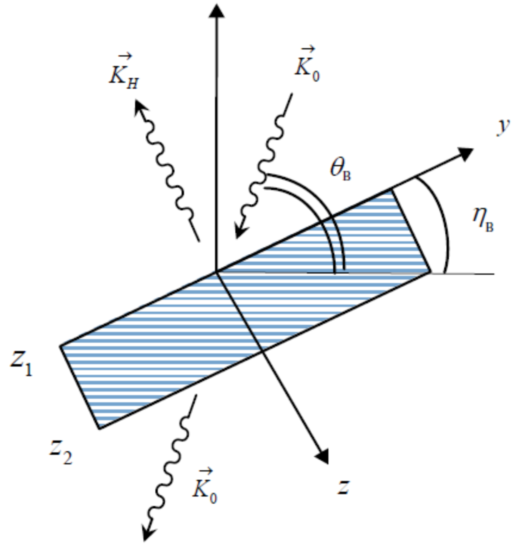

Y. Shvyd'ko and R. Lindberg, Phys. Rev. ST Accel. Beam, 15, 100702 (2012)

(Reflected) Bragg Diffraction

Bragg crystal

Incoming rays

Transmitted rays

Incoming radiation profile as a function of t

$$E_{in}(s) = E_0\, F(t)$$

Incoming radiation spectrum as a function of ω

FT

$$\mathcal{F}(\omega) = \frac{1}{2\pi}\int_{-\infty}^{\infty} F(t)\, e^{-i\omega t} dt$$

Reflected Bragg diffraction

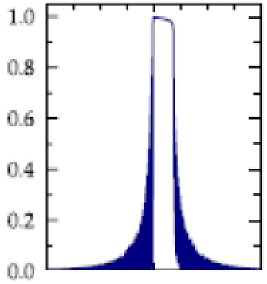

Reflected Bragg spectrum as a function of ω

$$\mathcal{g}_{0H}(\omega) = R_{0H}(\omega)\mathcal{F}(\omega)$$

Reflected Bragg radiation profile as a function of t

$$E_{0H}(t) = E_0\, G_{0H}(t)$$

Inverse FT

$$G_{0H}(t) = \frac{1}{2\pi}\int_{-\infty}^{\infty} \mathcal{g}_{0H}(\omega)\, e^{i\omega t} d\omega$$

Forward Bragg Diffraction

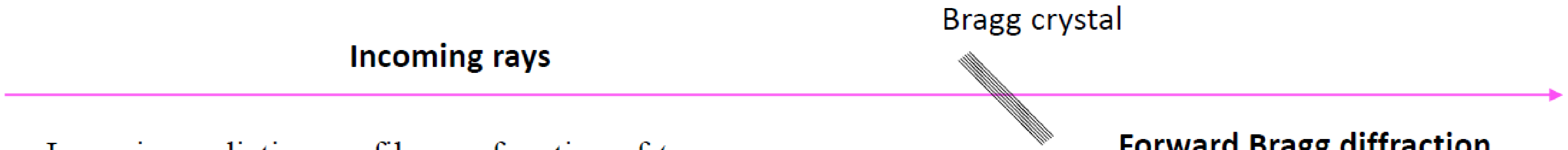

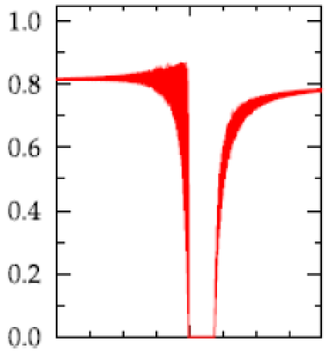

Incoming radiation profile as a function of t

$$E_{in}(s) = E_0 F(t)$$

FT

Incoming radiation spectrum as a function of ω

$$\mathcal{F}(\omega) = \frac{1}{2\pi}\int_{-\infty}^{\infty} F(t)\, e^{-i\omega t} dt$$

Forward Bragg spectrum as a function of ω

$$\mathcal{g}_{00}(\omega) = R_{00}(\omega)\mathcal{F}(\omega)$$

Inverse FT

Forward Bragg radiation profile as a function of t

$$E_{00}(t) = E_0 G_{00}(t)$$

$$G_{00}(t) = \frac{1}{2\pi}\int_{-\infty}^{\infty} \mathcal{g}_{00}(\omega)\, e^{i\omega t} d\omega$$

Monochromatic wake pulses

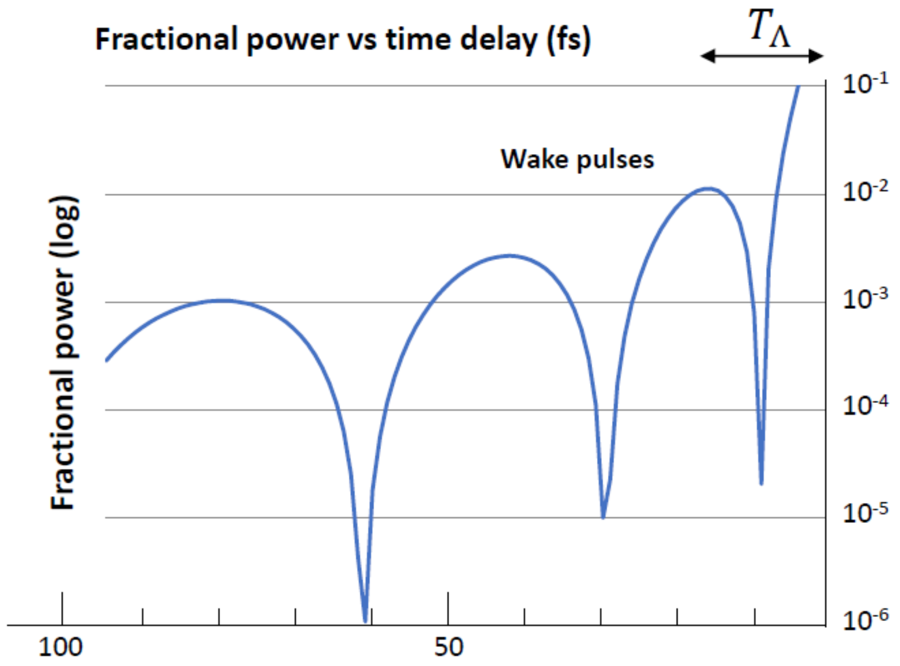

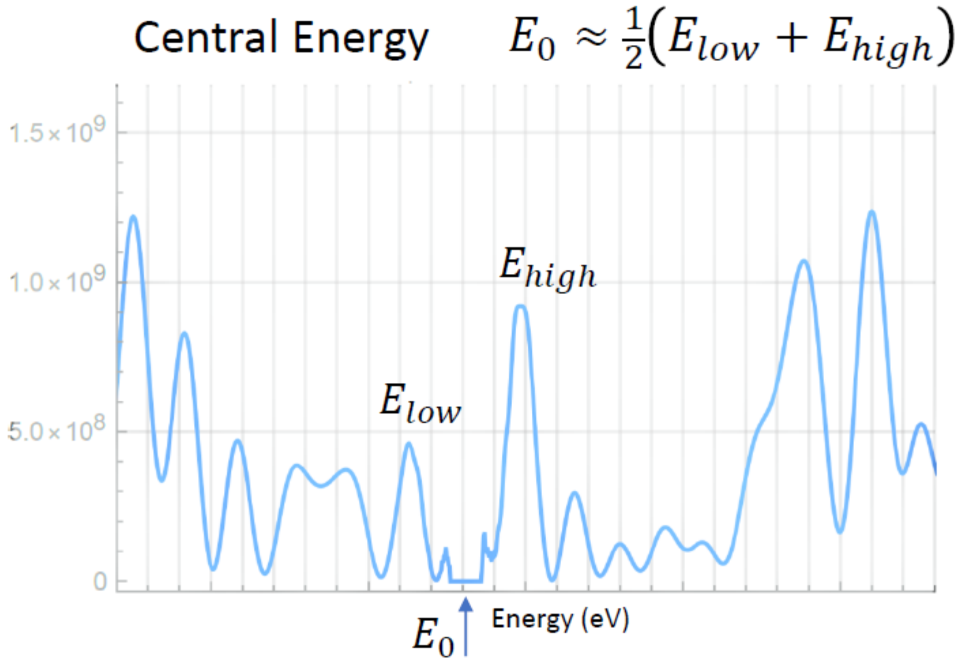

$$|G_{00}(t)|^2 \propto \left[\frac{1}{2T_0}\frac{J_1\left(\sqrt{\frac{t}{T_0}}\right)}{\sqrt{\frac{t}{T_0}}}\right]^2$$

First wake pulse delay

$$T_\Lambda = \frac{\Lambda_H}{2\pi\, c\, sin\theta_B}$$

Characteristic time

$$T_0 = \frac{\Lambda_H^2}{2\pi^2\, c\, d}$$

$\Lambda_H = \text{Extinction length}$

$d = \text{crystal thickness}$

Pathlength Delay & Offset in a Chicane

Chicane actions:

- wash out microbunching
- delay the electron bunch so it overlaps with one of the wake pulses
- offset the electron beam from the Bragg crystal

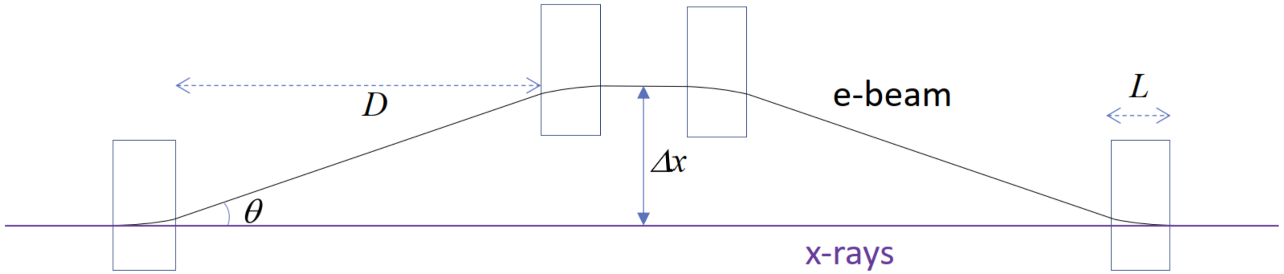

Difference between the electron and x-ray beam paths

$$\Delta L = \left(\frac{4}{3}L + 2D\right)\left(\frac{1}{cos\theta} - 1\right)$$

Chicane delay using small-angle approximation

$$\Delta L \approx \left(\frac{2}{3}L + D\right)\theta^2$$

Electron beam delay

$$\Delta t = \frac{\Delta L}{c} \qquad c = 0.3\ \mu m/fs$$

HXRSS Spectral Brightness Enhancement

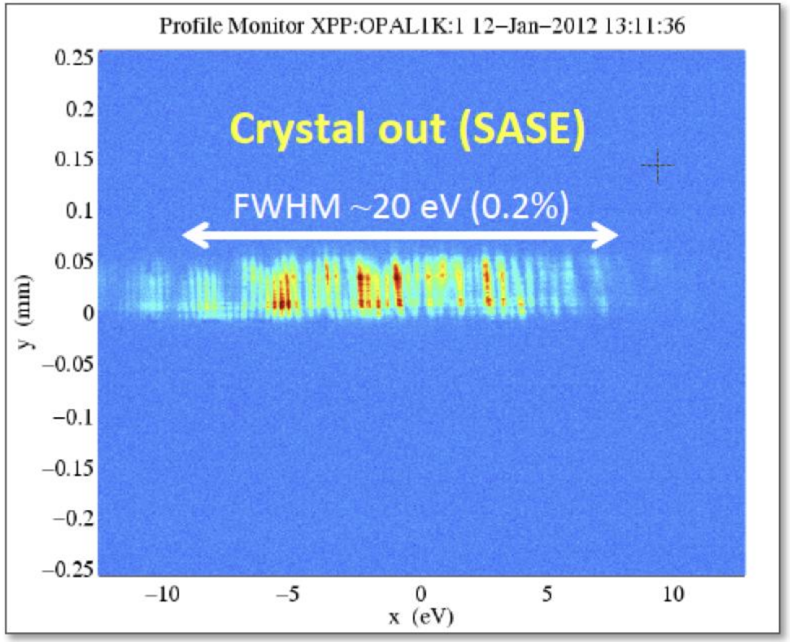

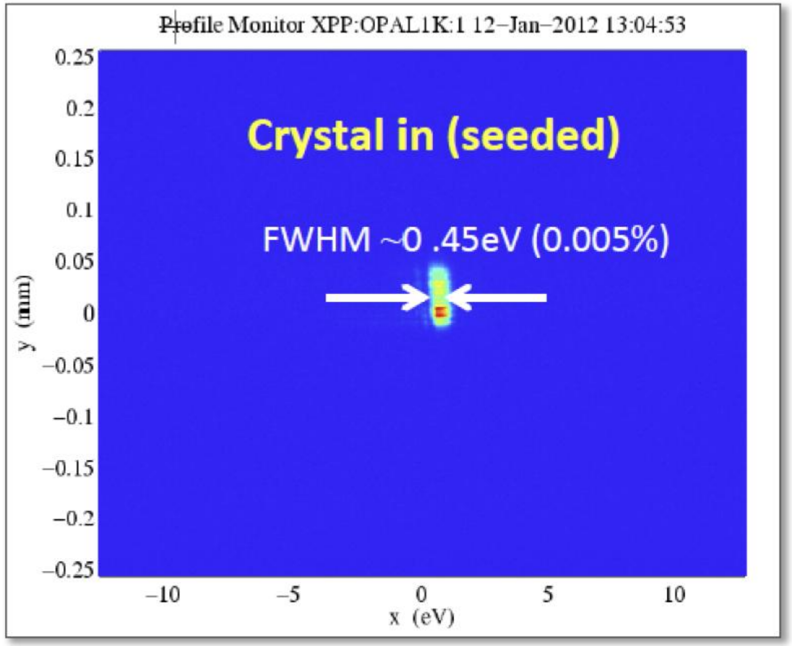

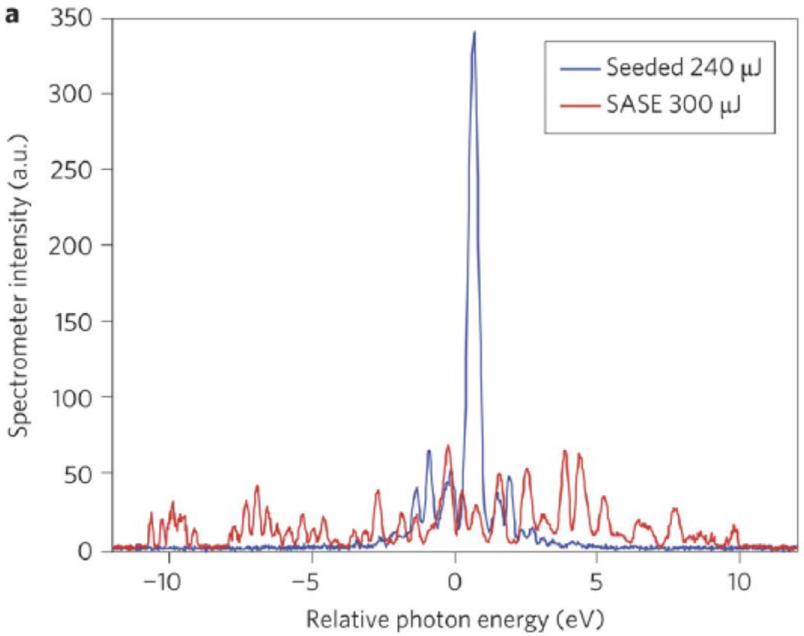

SASE relative BW

$$\frac{\Delta\omega}{\omega} \approx 1.5\rho \approx 2\times10^{-3}$$

HXRSS relative BW

$$\frac{\Delta\omega}{\omega} \approx 5\times10^{-5}$$

HXRSS brightness enhancement

$$\frac{\mathcal{B}_{SS}}{\mathcal{B}_{SASE}} \approx 30$$

Soft x-ray self-seeding

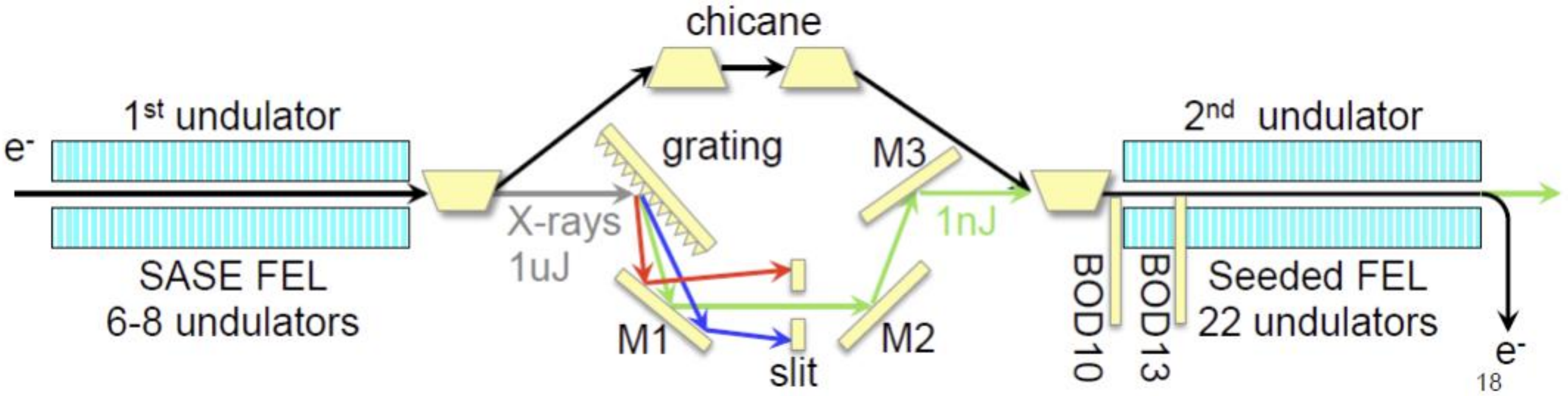

- Soft x-ray region
- Diffraction Grating: Resolution determines bandwidth
- Optical system: focusing and optical path return
- Chicane: smear bunching, delay, offset
- Complex system and unstable

Cavity based XFEL

Cavity based XFEL

- Originally, cavity-based FEL is used for **FELO** (low gain) in the range from infrared to THz FEL.
- Recently, due to the development of crystallography, CBXFEL focus on X-ray regime.
- Key: Bragg diffraction.
- Cavity-based FELs include XFEL oscillators (XFELOs) and X-ray regenerative amplifier FELs (RAFELs).
- **XFELO:** Low gain regime, short undulator, low-quality electron beam, many passes
- **RAFEL:** High gain regime, long undulator, high-quality electron beam, a few passes
- In fact, we usually refer to them as XFELO or CBXFEL collectively.

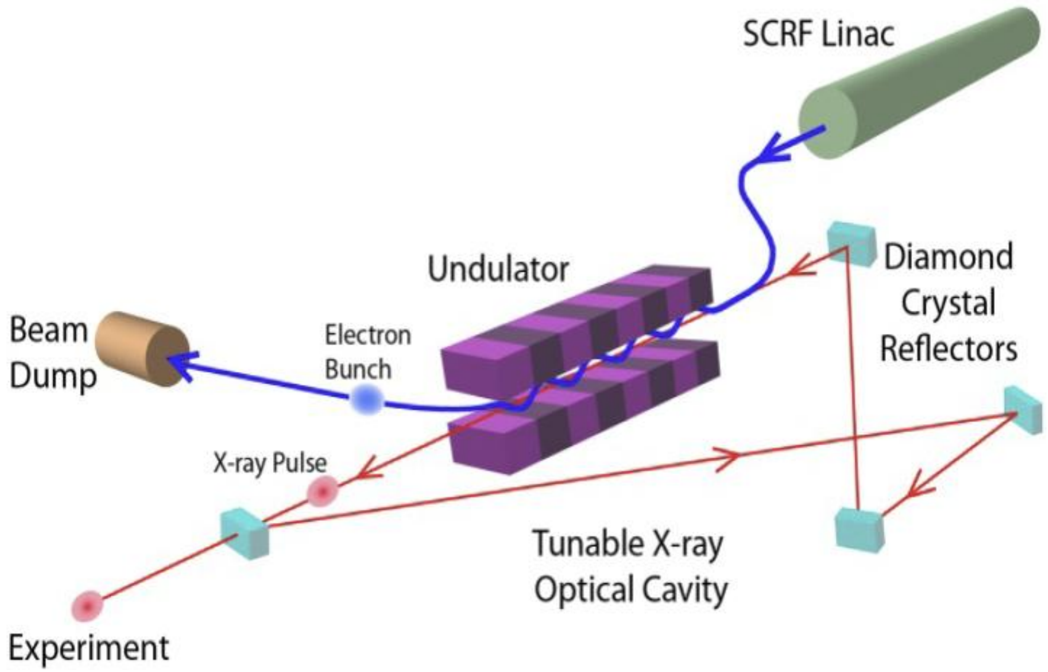

XFELO demonstrated at European-XFEL in May, 2025

X-ray FEL Oscillators

- Small-signal gain (G_{SS})

$$P_{out} = (1 + G_{ss})P_{in}$$

- Saturated gain = Cavity loss

$$P_{out} = (1 + L)P_{in}$$

- Optical cavity

$$L_{cav} = \frac{c}{f_b}$$

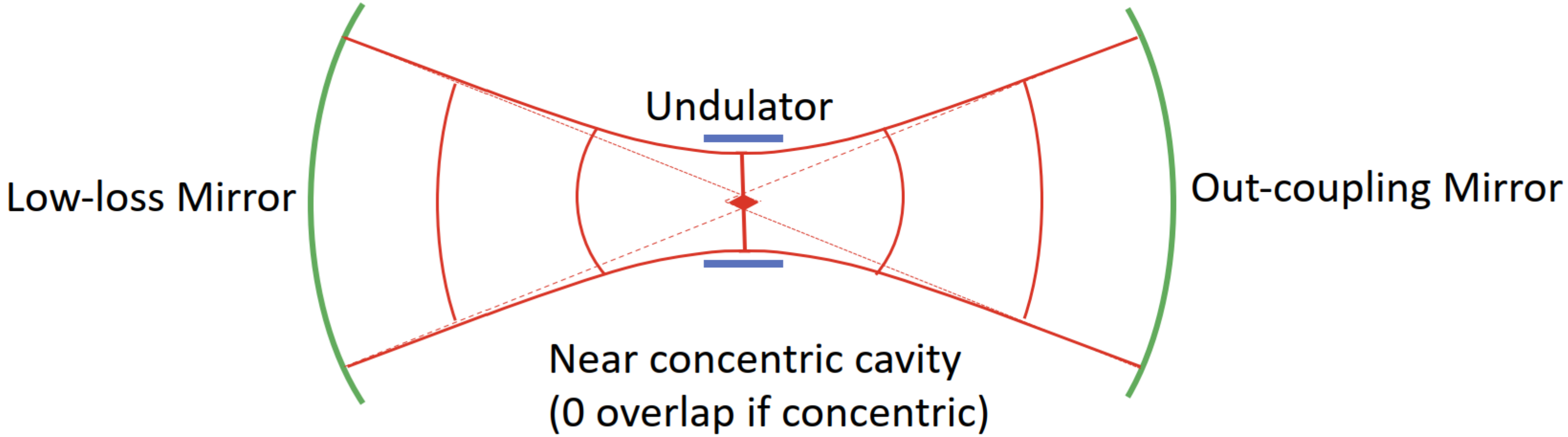

- Cavity loss = Out-coupling + Mirror absorption + Diffraction

Some detail about FELO

Pass *1*: spontaneous emission

$$P_1 = P_0$$

Pass *i*:

$$P_i = P_{i0}(1+g_i),\quad i>1$$

$$P_{i0} = P_{i\text{-}1}(1-\alpha)$$

P_{i0}: **Pass *i*'s initial power intensity**

P_i: **Pass *i*'s end power intensity**

g_i: **Pass *i*'s power gain**

α: **Pass *i*'s cavity loss**

Pass *m*'s intensity:

$$P_m = P_{\text{m-1}}(1-\alpha)(1+g_m) = P_0(1-\alpha)^{m-1}\prod_{i=2}^{m}(1+g_i)$$

Pass *i*'s net gain:

$$g_{i,net} = (P_i - P_{\text{i-1}})/P_{\text{i-1}} = (1-\alpha)g_i - \alpha$$

Some detail about FELO

- Low gain: undulator length < 3 gain length
- Initial gain ~ small signal gain g_{ss}
- As the electric field is amplified, the FEL gain gradually decreases until the balance between the gain and cavity loss, i.e. saturation
- At saturation, the net gain is zero:

$$g_{s,net} = (1-\alpha)g_s - \alpha = 0$$

$$\Rightarrow g_s = \alpha / (1-\alpha)$$

- For the oscillator:

$$\alpha / (1-\alpha) \le g_i \le g_{ss}$$

Some detail about FELO

- At saturation, the single pass gain equals cavity loss

$$\Delta P_+ = \eta_s P_e = \Delta P_- = \alpha P_s$$

$$\Rightarrow P_s = \eta_s P_e / \alpha \le \eta_{\max} P_e / \alpha = P_e / \alpha 2N_u$$

- The condition for the above equal sign to hold is that **saturation power of the balance state** is equal to **small signal saturation power**.

$$\eta_s = \eta_{\max} = 1/2N_u$$

- And the total passes: $M \approx \dfrac{2\ln(P_s/P_0)}{g_{ss} - \alpha - g_{ss}\alpha} \sim 100$

- Saturation power in the cavity: $P_{s\_\max} = P_e / \alpha 2N_u$

- Assuming out-coupling power = cavity loss, so $P_{out} = \alpha P_{s\_\max} = P_e / 2N_u$

中國科學院 上海高等研究院
SHANGHAI ADVANCED RESEARCH INSTITUTE, CHINESE ACADEMY OF SCIENCES

X-ray RAFEL with Bragg Reflectors

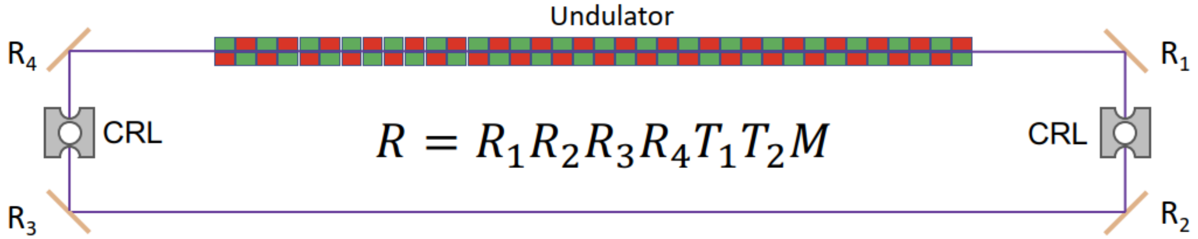

$$R = R_1 R_2 R_3 R_4 T_1 T_2 M$$

$R_1 R_2 R_3 R_4$ = Reflectivity of the Bragg reflectors within $\Delta\theta$

$T_1 T_2$ = Transmittivity of the two CRLs

M = Fraction of the return power that matches the FEL mode

RAFEL power in the n^{th} pass

$$P_n(z) = \frac{R P_{n-1}}{9} e^{\frac{z}{L_G}}$$

Bragg angle has to be slightly less than 45°

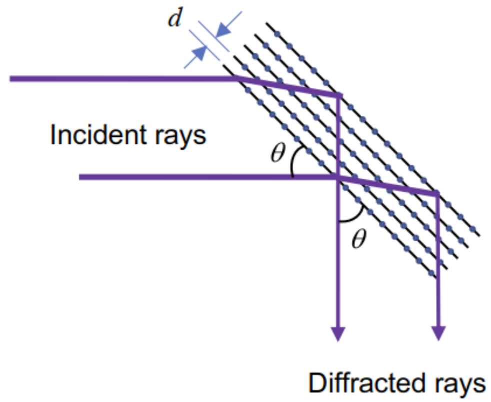

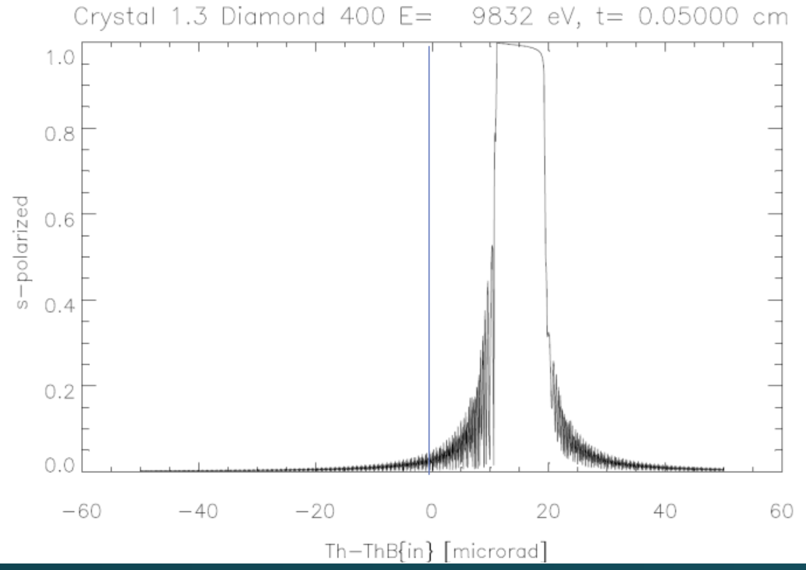

SASE and CBXFEL

	SASE	XRAFEL	XFELO
Peak Power	~10 GW	~50 GW	~100 MW
Average Power	100 W (at ~ 1 MHz)	10 W (at ~ 10 kHz)	20 W (at ~ 1 MHz)
Spectral Bandwidth	~10 eV	~0.1 eV	~1 meV
Pulse Length	~1-100 fs	~20 fs	~1 ps
Stability	Poor	Excellent	Excellent
Poor	Excellent	Excellent	Excellent
Transverse Mode	Defined by the gain guiding	Defined by the gain guiding	Defined by the optical cavity

External seedings: HGHG and EEHG

中国科学院上海高等研究院
SHANGHAI ADVANCED RESEARCH INSTITUTE, CHINESE ACADEMY OF SCIENCES

Principle of HGHG FEL

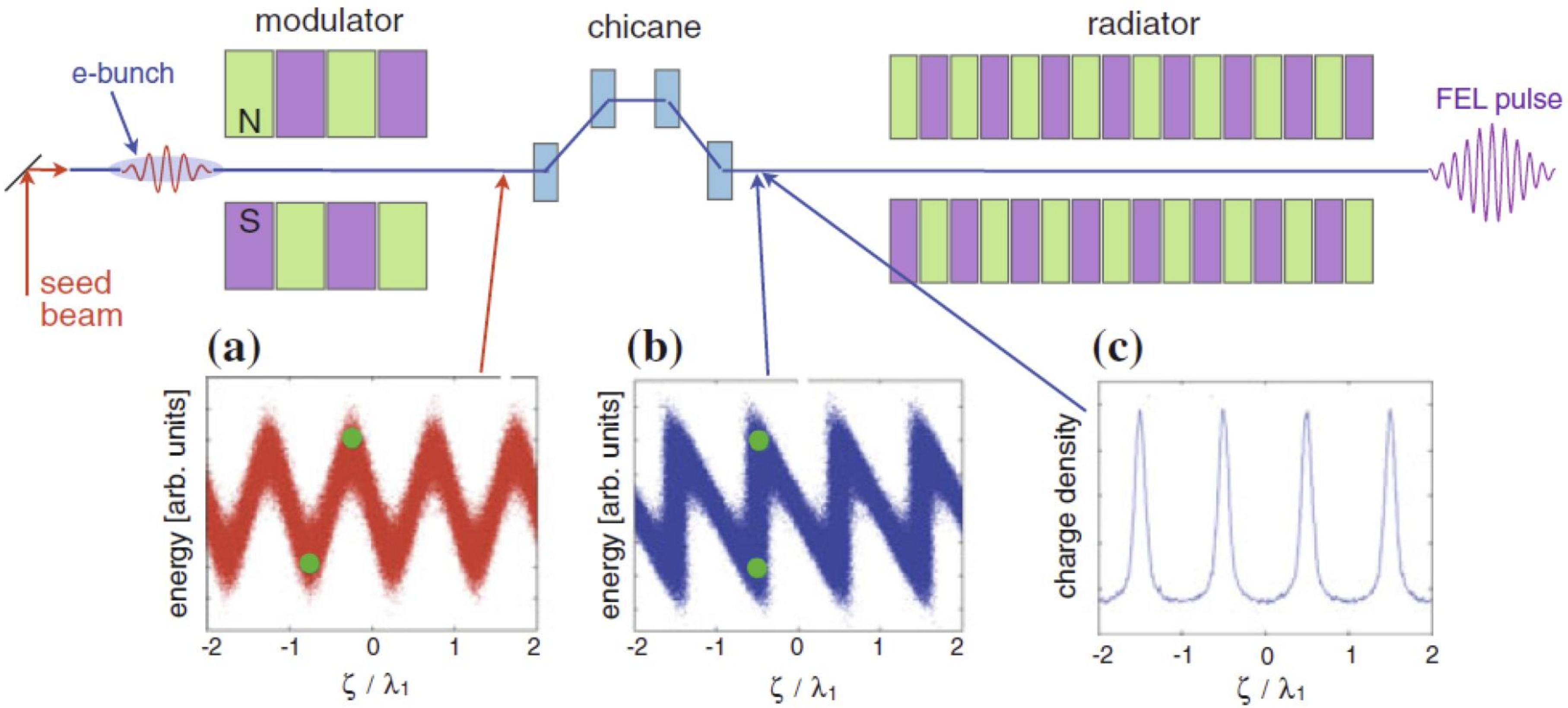

HGHG uses an external laser to modulate the electron energy in the **modulator**, followed by a **chicane** to converts the energy modulations into density modulations, and finally the bunched beam with high Fourier coefficients radiates coherently at a harmonic frequency in the **radiator**.

HGHG: energy modulation from seed laser

- According to the low gain FEL theory, a seed laser interacts with an electron beam in a short undulator and generates energy modulation. Reviewing perturbation analysis, the 1st order is the modulation term

$$\epsilon\eta_1(z) = -\frac{eE_0K[\mathrm{JJ}]}{2\gamma_r^2mc^2}z\sin\phi_0$$

- The energy modulation amplitude introduced by seed laser in the modulator

$$\Delta\eta = \frac{eE_0K[JJ]}{2\gamma_r^2mc^2}L_u = \frac{K[JJ]}{\gamma_r^2}\sqrt{\frac{L_u^2}{\sigma_r^2}\frac{e^2}{4\pi\epsilon_0mc^2}\frac{P}{mc^3}}$$

$$= \frac{K[JJ]}{\gamma_r^2}\frac{L_u}{\sigma_r}\sqrt{\frac{P}{P_{rel}}} \quad \rightarrow \quad \frac{2\pi K[JJ]}{\gamma_r^2}\sqrt{\frac{L_u}{\lambda_l}\frac{P}{P_{rel}}}$$

- $P_{rel} = mc^3/r_e \approx 8.7\ \mathrm{GW}$, $\sigma_r^2 = \lambda_l Z_R/4\pi$, $Z_R \sim L_u/\pi$

HGHG: Initial phase space

Suppose the initial longitudinal phase space could be expressed as a normalized gaussian function of:

$$\mathfrak{F}_0\left(\gamma, s\right) = \frac{1}{\sqrt{2\pi}\sigma_\gamma} e^{-\delta\gamma^2/2\sigma_\gamma^2}$$

Where $\delta\gamma = \gamma - \gamma_0$. In order to make the notations clearer, we introduce $p = \delta\gamma/\sigma_\gamma$, $A = \Delta\gamma/\sigma_\gamma$ and $B = R_{56}k\sigma_\gamma/\gamma$ with $\Delta\gamma$ the energy modulation amplitude, R_{56} the strength of chicane and k the wavelength number of seed laser. Then we get the initial distribution function with the form of:

$$\mathfrak{F}_0(p, \xi) = \frac{1}{\sqrt{2\pi}} e^{-p^2/2}$$

where $\xi = ks$ is longitudinal phase.

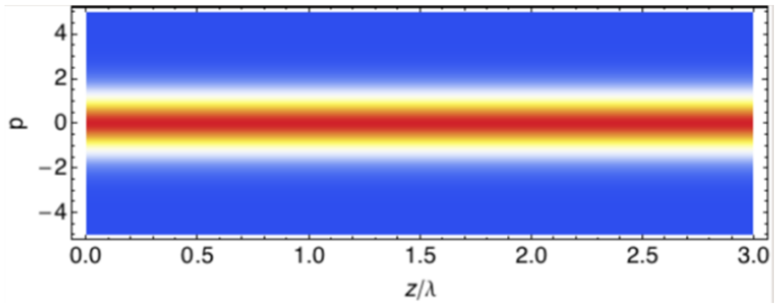

HGHG: energy and density modulations

After modulated by the external seed laser, say the reduced energy modulation amplified is A, i.e. $p' = p + A\sin\xi$; such kind of energy modulation will lead the longitudinal density modulation by chicane, i.e. $s' = s + R_{56}\delta\gamma/\gamma \Rightarrow \xi' = \xi + Bp$, thus the longitudinal distribution after chicane could be written as:

$$\mathfrak{F}_1\left(p', \xi'\right) = \frac{1}{\sqrt{2\pi}} e^{-(p' - A\sin(\xi' - Bp'))^2}$$

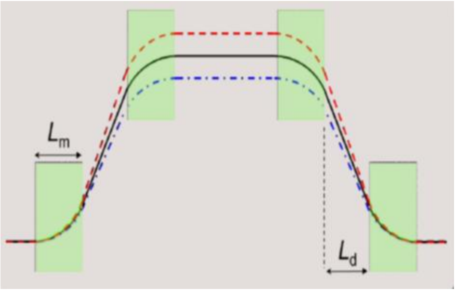

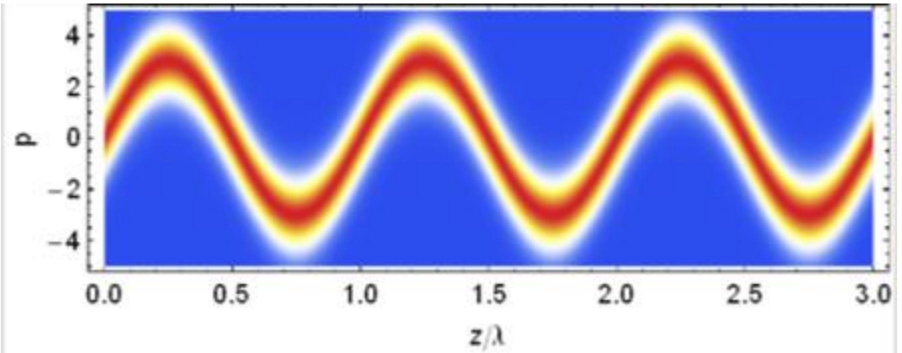

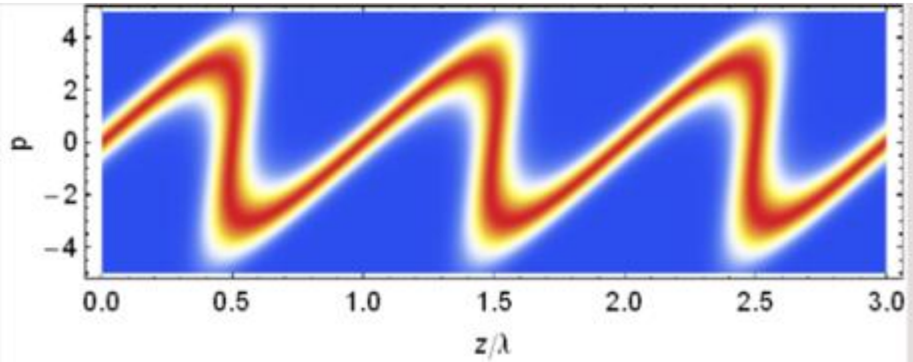

HGHG： bunching factor

The bunching factor yields as:

$$b_n = \left|\overline{e^{-in\xi}}\right| = \left|\int e^{-in\xi'} \mathfrak{F}_1(p', \xi')\, \mathrm{d}p'\, \mathrm{d}\xi'\right|$$

$$\begin{aligned}
b_n &= \left|\int e^{-in\xi'} \mathfrak{F}_1(p', \xi')\, \mathrm{d}p'\, \mathrm{d}\xi'\right| \\
&= \left|\int e^{-in(\xi + B(p + A\sin\xi))} \mathfrak{F}_0(p, \xi)\, \mathrm{d}p\, \mathrm{d}\xi\right| \\
&= \left|\frac{1}{\sqrt{2\pi}} \int \mathrm{d}p\, \mathrm{d}\xi e^{-\frac{1}{2}(p+inB)^2 - \frac{1}{2}n^2B^2} e^{-in\xi} e^{-inAB\sin\xi}\right| \\
&= \left|\frac{1}{\sqrt{2\pi}} \int \mathrm{d}p\, \mathrm{d}\xi e^{-\frac{1}{2}(p+inB)^2 - \frac{1}{2}n^2B^2} e^{-in\xi} \sum_{m=-\infty}^{\infty} J_m(nAB) e^{-im\xi}\right| \\
&= \left|e^{-\frac{1}{2}n^2B^2} \int \mathrm{d}\xi \sum_{m=-\infty}^{\infty} J_m(nAB) e^{-i(m+n)\xi}\right| \\
&= e^{-\frac{1}{2}n^2B^2} J_n(nAB)
\end{aligned}$$

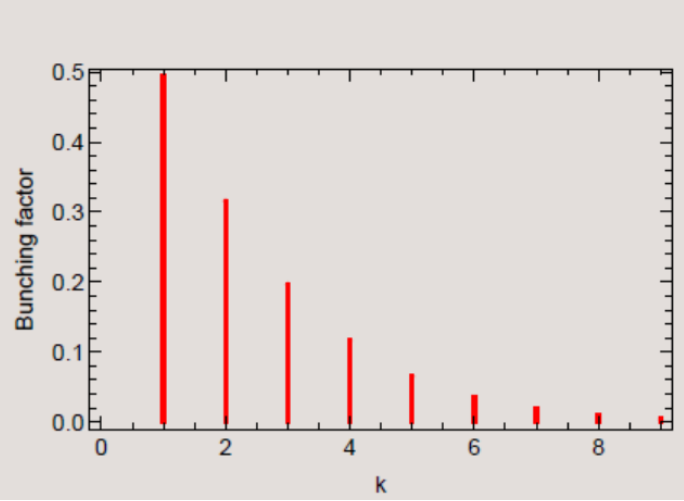

$$b_n = e^{-\frac{1}{2}n^2B^2} J_n(nAB)$$

Optimal solution for maximal bunching:

$\{AB\}_{\max} \approx 1.2$

Principle of EEHG FEL

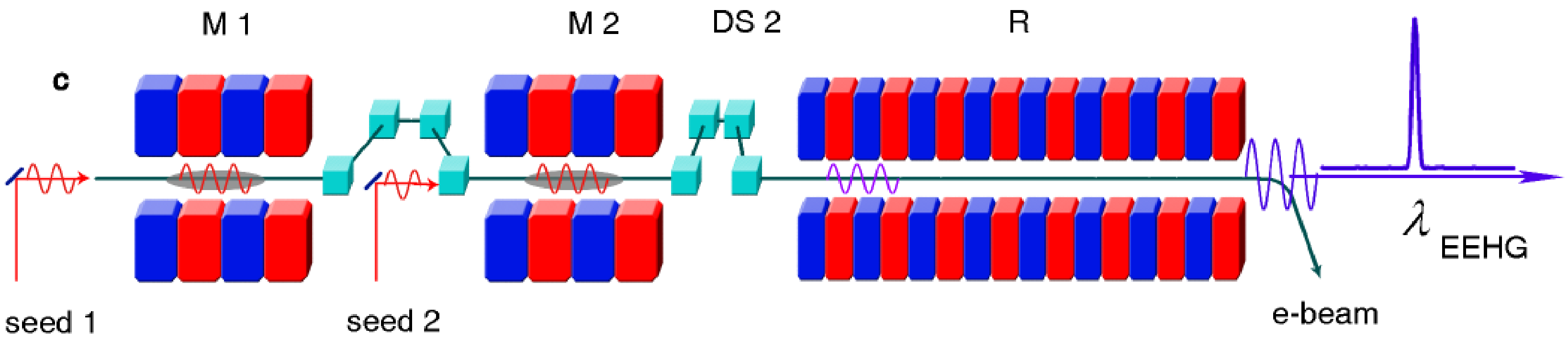

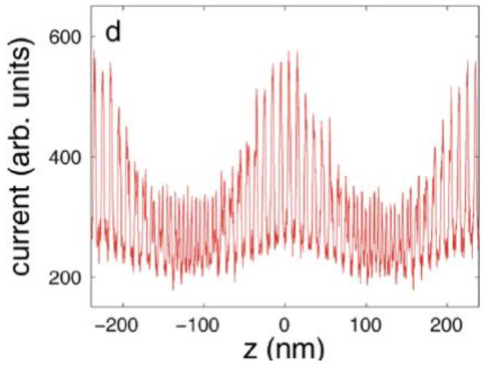

G. Stupakov, PRL (2009)

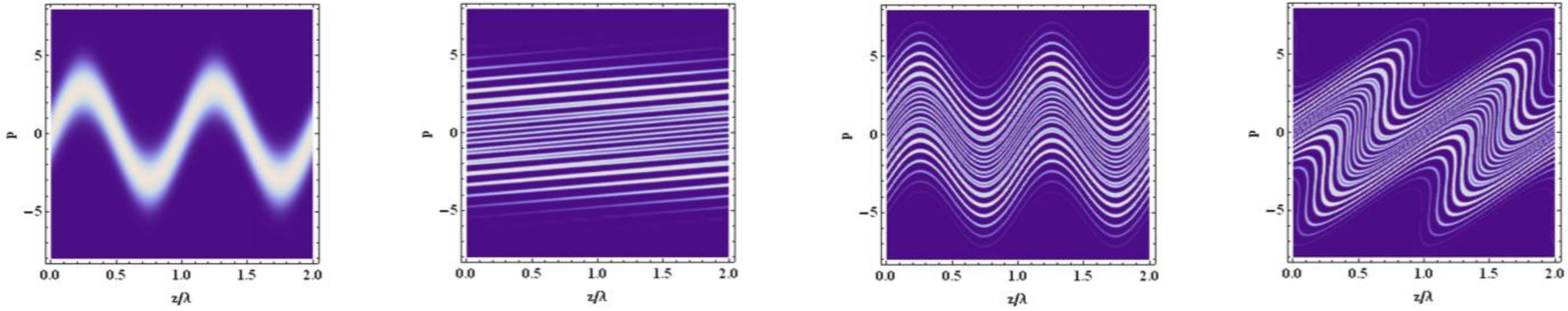

EEHG: phase space

- First energy modulation: $p' = p + A_1 \sin\theta\,,$
- After first chicane: $\theta' = \theta + B_1 p'\,.$
- Second energy modulation $p'' = p' + A_2 \sin(\kappa\theta' + \psi)$
- After second chicane $\theta'' = \theta' + B_2 p''$

$$f_0(\theta, p) = \frac{1}{\sqrt{2\pi\theta_b}} \exp(-p^2/2)$$

$$b_h = \int dp'' d\theta''\; f(p'', \theta'') e^{-ih\theta''} = \int_{-\infty}^{\infty} dp \int_{-\theta_b/2}^{\theta_b/2} d\theta\; f_0(p) \exp[-ih\theta''(\theta, p)]$$

EEHG: bunching factor

We can substitute Eq. (6.39) into the last expression to obtain the bunching factor for $h = m\kappa + n$ as

$$b_{n,m} = e^{im\psi} e^{-[(m\kappa+n)B_2+nB_1]^2/2} \times J_m\left[-(m\kappa+n)A_2B_2\right] J_n\left\{-A_1\left[nB_1+(m\kappa+n)B_2\right]\right\} . \quad (6.43)$$

The Gaussian prefactor will significantly suppress the bunching unless its argument is small; if we use the same type of device for both dispersive section (e.g., two chicanes), than B_1 and B_2 will have the same sign and the bunching will be insignificant unless n and m have opposites signs. Further analysis shows that the magnitude of the bunching factor attains its maximum when $n = \pm 1$ and rapidly decreases as the absolute value of n increases; we therefore take $n = -1$ and $m > 0$ in Eq. (6.39) for a particular harmonic number $h = m\kappa - 1$. Note that because only a single phase $e^{im\psi}$ contributes to the harmonic number h, any phase difference between the two lasers does not affect the magnitude of the bunching; in other words, the harmonic bunching of an optimized EEHG device is not sensitive to the relative phase between the two lasers. The relevant expression for the maximal bunching at harmonic $h = m\kappa - 1$ is

$$|b_{-1,m}| = \left|J_m\left[(m\kappa-1)A_2B_2\right] J_1(A_1\varpi)\right| e^{-\varpi^2/2} , \quad (6.44)$$

where $\varpi = B_1 - (m\kappa - 1)B_2$.

Optimal solution:

$$b_{\max} = \frac{0.39}{m^{1/3}}$$

中国科学院上海高等研究院
SHANGHAI ADVANCED RESEARCH INSTITUTE, CHINESE ACADEMY OF SCIENCES

Seeded FEL: FEL performances

- During the first two gain length, coherent harmonic generation (CHG) without high gain:

$$P_{coh} = \frac{Z_0 I_p^2 K^2 b_k^2 [JJ]^2}{32\pi \Sigma_A \gamma^2} (2L_G)^2$$

- $Z_0 = 377\ \Omega$ is vacuum impedance and I_p is peak current.
- After the first two gain length, high gain regime.
- When calculating the 3D gain length, it is necessary to consider the energy spread added by modulation. The slice energy spread and the saturation power can be estimated as:

$$\sigma_{\gamma 2} = \sigma_\gamma \sqrt{1 + \frac{A^2}{2}} \qquad P_{sat} = 1.6\rho \times \left(\frac{L_{G1D}}{L_{G3D}}\right)^2 \frac{\gamma m_e c^2 I_p}{e}$$

- And the saturation length is

$$L_{sat} = L_{G3D}\left[\ln\left(\frac{P_{sat}}{P_{coh}}\right) + 2\right]$$

HGHG and EEHG bunching factors

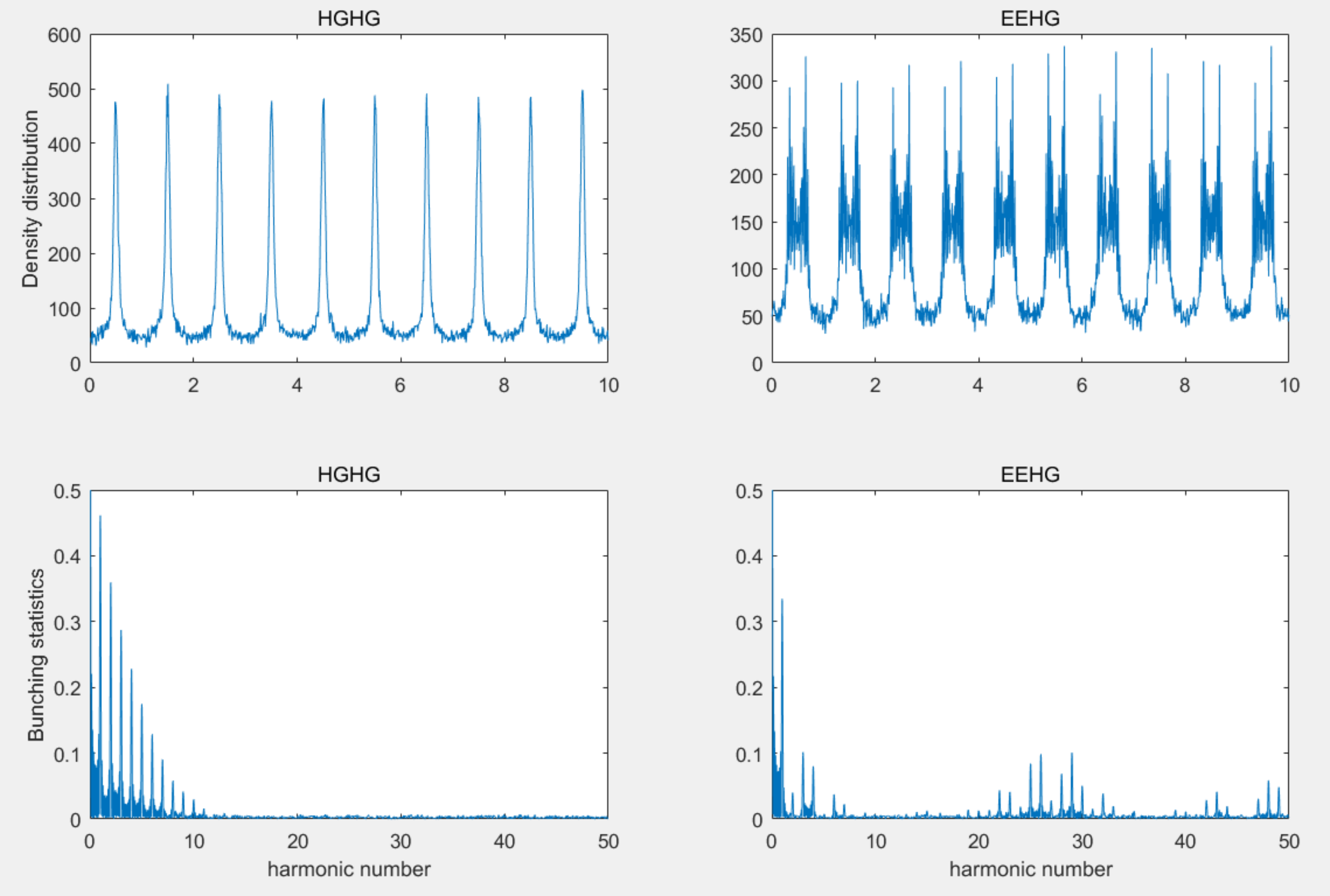

- HGHG produces narrow-linewidth radiation at the harmonic of the seed laser. HGHG is sensitive to energy spread as well as phase and frequency changes in the laser.

- EEHG is an attractive technique to the generation of ultra-high harmonic from the laser-driven harmonic FEL.

XFEL operations worldwide

FLASH	SASE (EEHG)
LCLS (+II+HE):	SASE, self-seeding, (EEHG, XFELO)
SACLA	SASE, self-seeding
FERMI	HGHG, HGHG cascading (EEHG, EEHC)
PAL-XFEL	SASE, self-seeding
European-XFEL	SASE, self-seeding (XFELO)
Swiss-FEL	SASE, self-seeding (EEHG)
SXFEL	SASE, HGHG, EEHG, EEHC, …
SHINE	SASE, self-seeding, EEHG, EEHC, …
S3FEL	EEHG, EEHC, …
…	…

Homework

- Derive the electron motion equations and resonance condition in an undulator.
- Derive the bunching factor of HGHG.
- Assume an FEL facility with 4 GeV beam energy, 1 kA peak current, and 0.5 mm*mrad normalized slice emittance. The average beta function is 10 m in the undulator with 40 mm undulator period length. Considering 3 nm SASE generation, please calculate undulator parameter, Pierce parameter, gain length, saturation length, and saturation power under 1D theoretical condition.

Backup materials

Focusing in long undulators

In a FODO lattice, the electron beam radii in x and y oscillate between a maximum and minimum values set by the β functions and the un-normalized emittance in x and y. We consider the case where $\varepsilon_x = \varepsilon_y$ and $\beta_x > \beta_y$

$$\sigma_{max} = \sqrt{\beta_x \varepsilon_x}$$

$$\sigma_{min} = \sqrt{\beta_y \varepsilon_y}$$

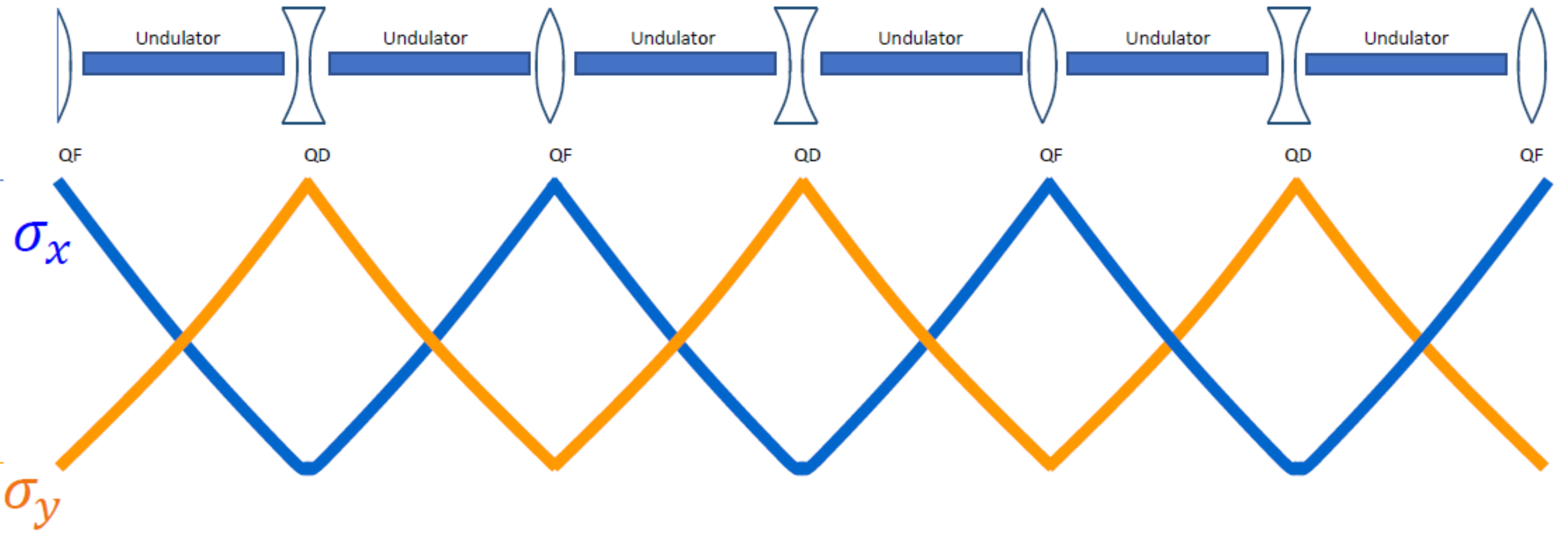

Electron beam rms angle

$$\sigma_{x'} = \sqrt{\varepsilon_x \frac{(1+\alpha_x^2)}{\beta_x}} = \sigma_{y'} = \sqrt{\varepsilon_y \frac{(1+\alpha_y^2)}{\beta_y}}$$

Natural focusing in an undulator

- The undulator field is only valid very near the y = 0 plane in 1D theory because it does not satisfy the vacuum Maxwell equations in 3D. An exact solution of Maxwell's equations describing a planar undulator with flat poles is

$$\boldsymbol{B}(\boldsymbol{x};z) = -B_0\cosh(k_u y)\sin(k_u z)\hat{y} - B_0\sinh(k_u y)\cos(k_u z)\hat{z}.$$

- Thus, we can find that

$$x' \equiv \frac{dx}{dz} = \frac{dx/dt}{dz/dt} \approx \frac{K}{\gamma}\cosh(k_u y)\cos(k_u z) + x'(0).$$

$$y'' \approx -\frac{K^2 k_u}{\gamma_r^2}\cos^2(k_u z)\sinh(k_u y)\cosh(k_u y)$$

$$\approx -\left(\frac{K k_u}{\gamma_r}\right)^2 \cos^2(k_u z) y$$

The harmonic oscillator equation →

$$y'' = -k_{n0}^2 y$$

$$k_{n0} = \frac{K k_u}{\sqrt{2}\gamma} \equiv \frac{1}{\beta_n}.$$

FODO lattice in undulators

- Strong focusing + natural focusing

SHINE

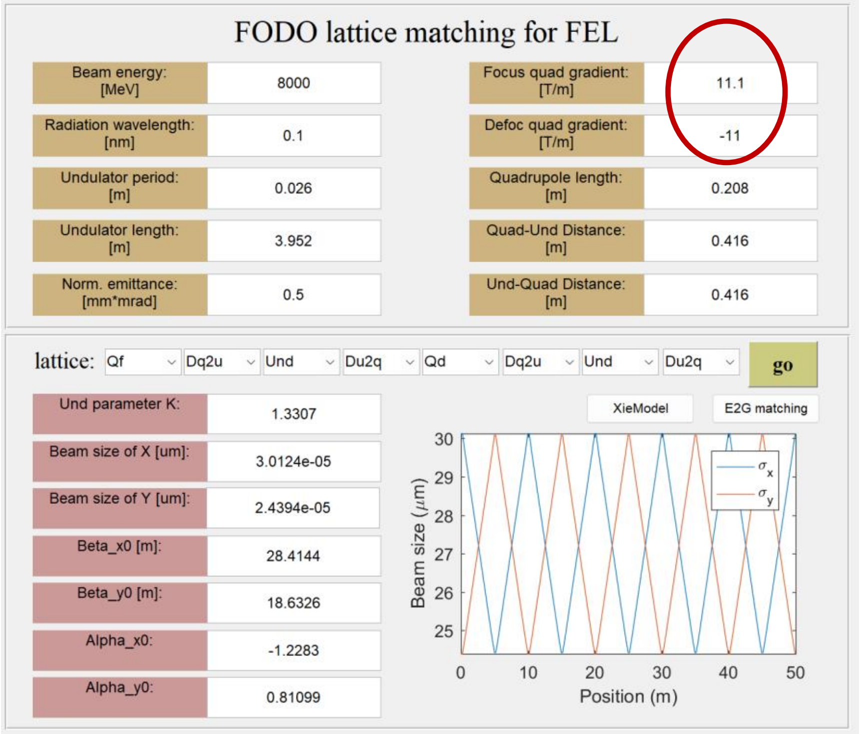

No impact of natural focusing

SHINE:

QF=2.3T
QD=-2.3T

SXFEL:

QF=0.6T
QD=0.6T

SXFEL

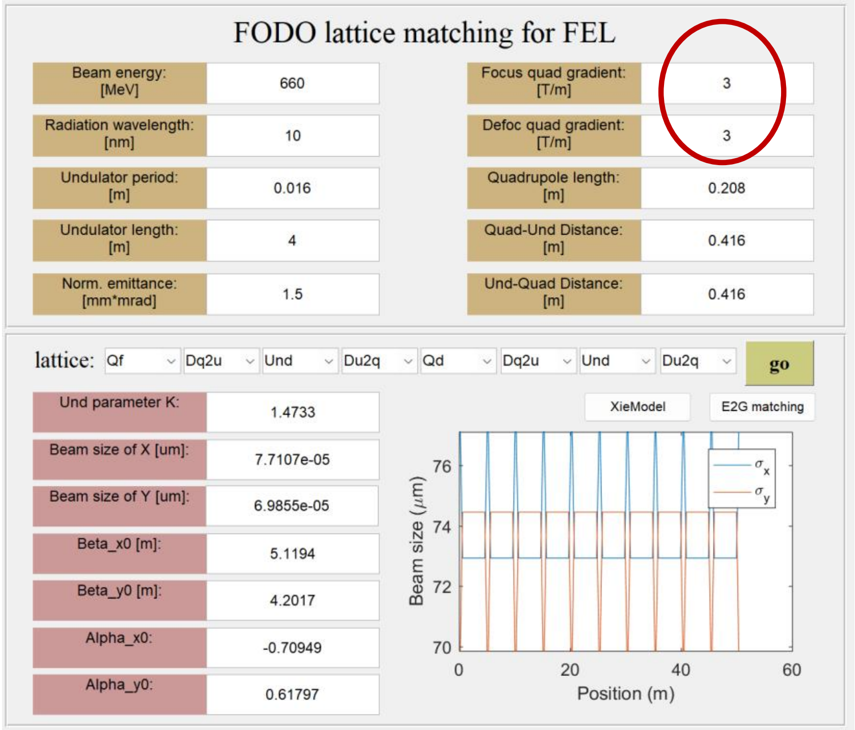

Heavy impact of natural focusing

HGHG&EEHG advances

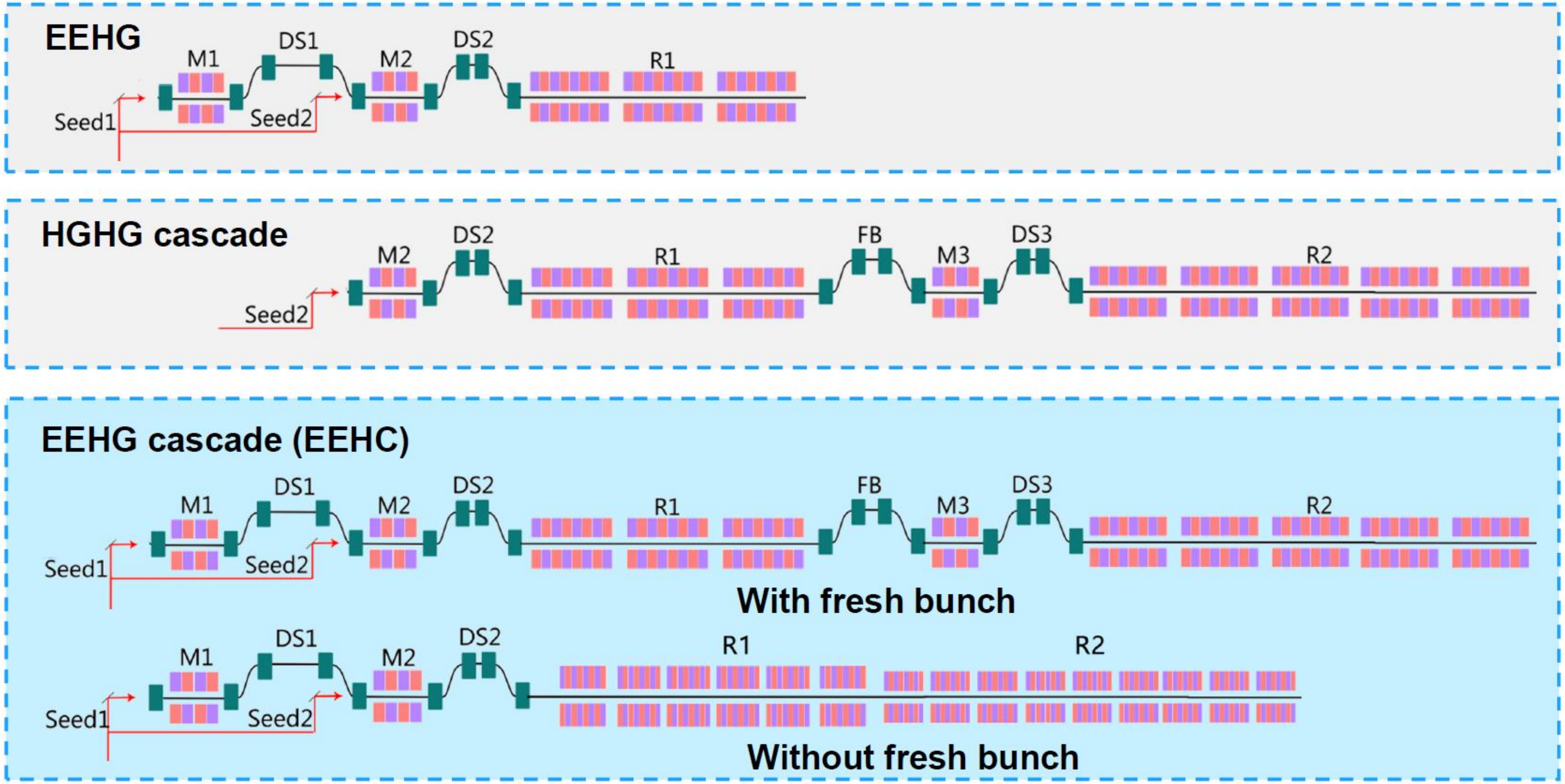

SM&DE-HGHG/EEHG

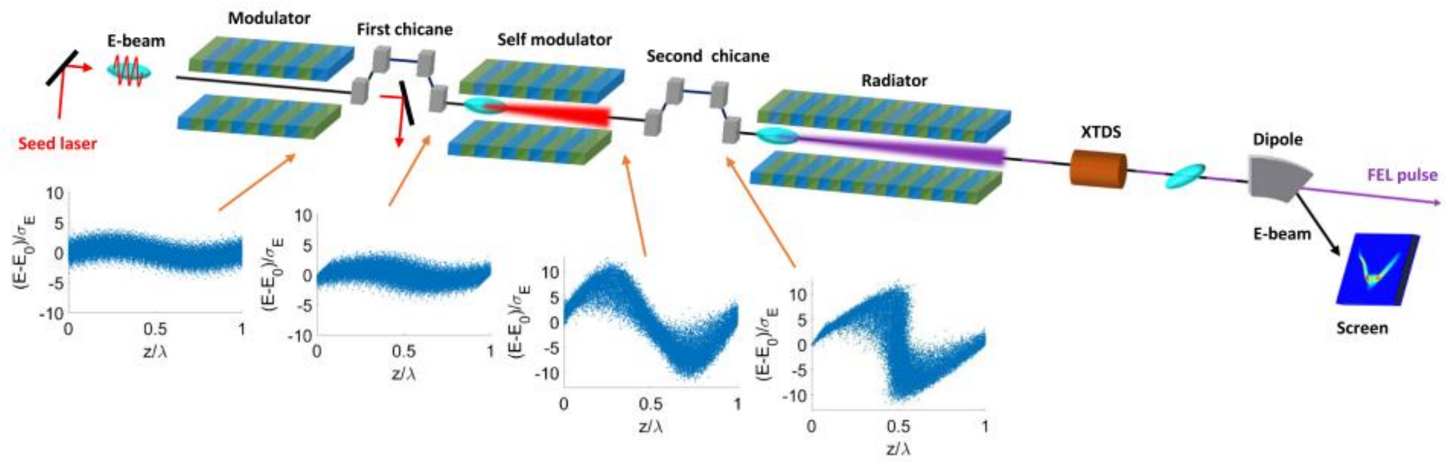

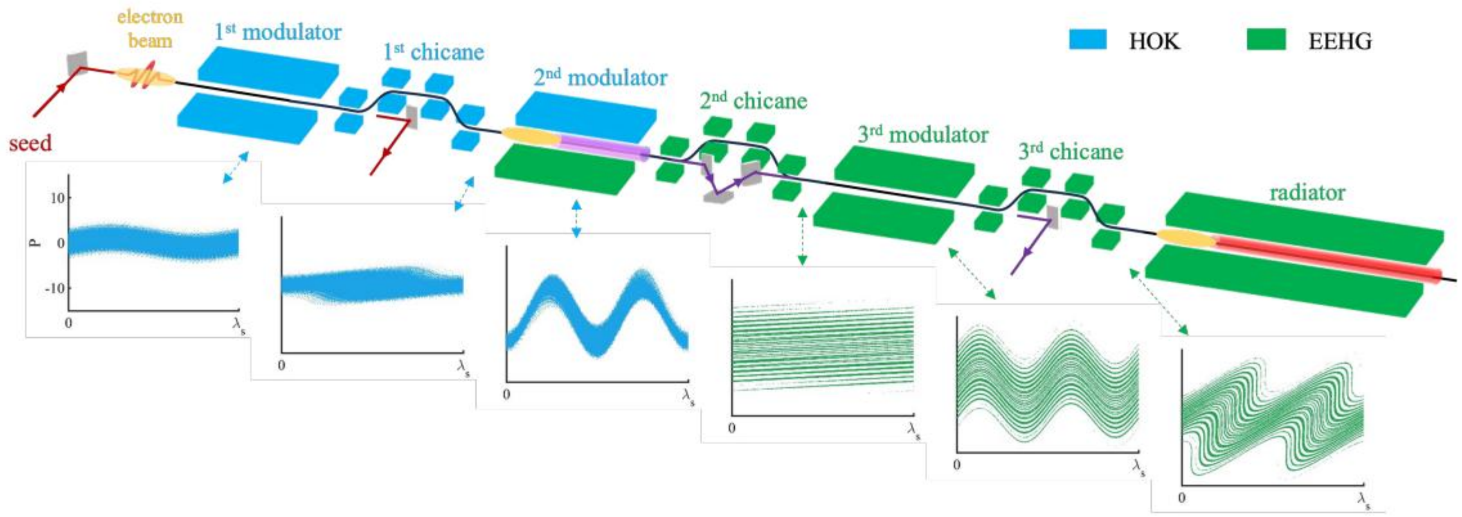

Transverse Gradient Undulator

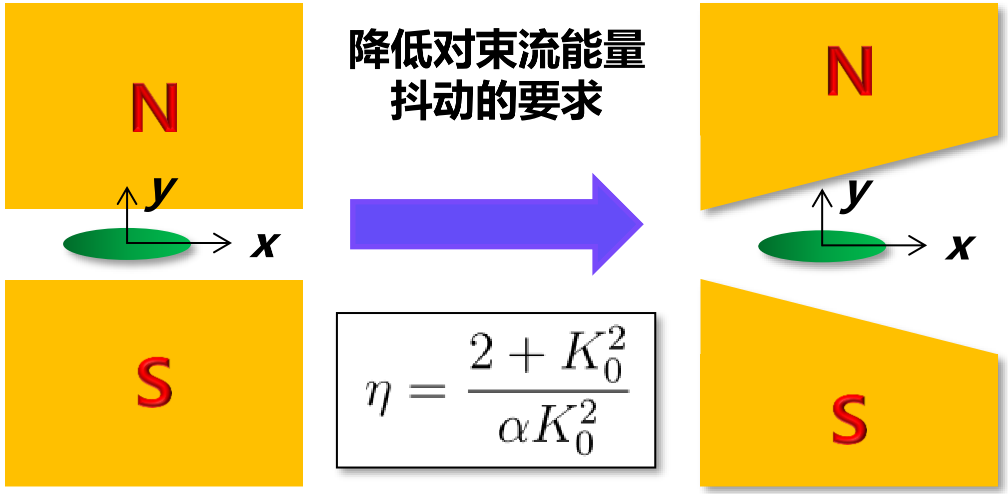

$$\eta = \frac{2 + K_0^2}{\alpha K_0^2}$$

- T. I. Smith, et al., Journal of Applied Physics, **50** (1979) 4580.
- N. Kroll, et al., IEEE Journal of quantum Electronics, **17** (1981) 1496.
- Z. Huang, et al, Physical Review Letter, **109** (2012) 204801.

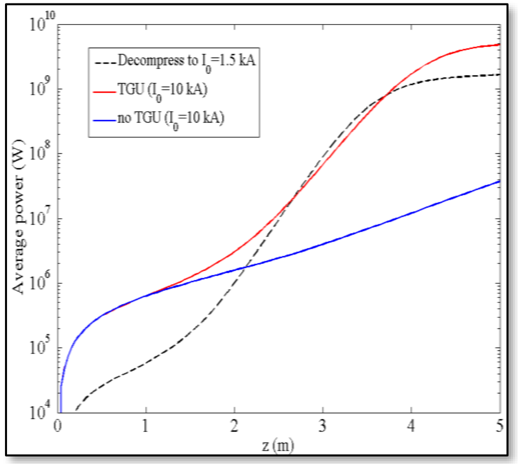

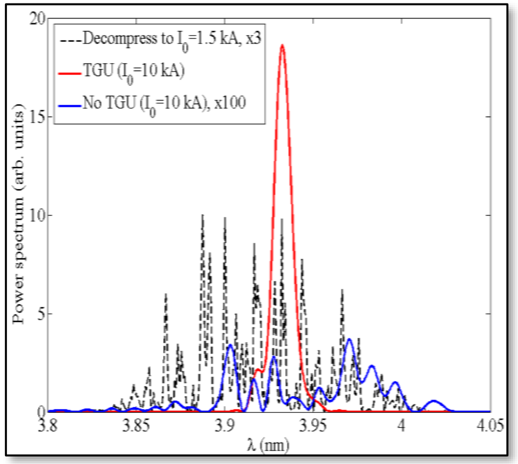

Phase-merging effect

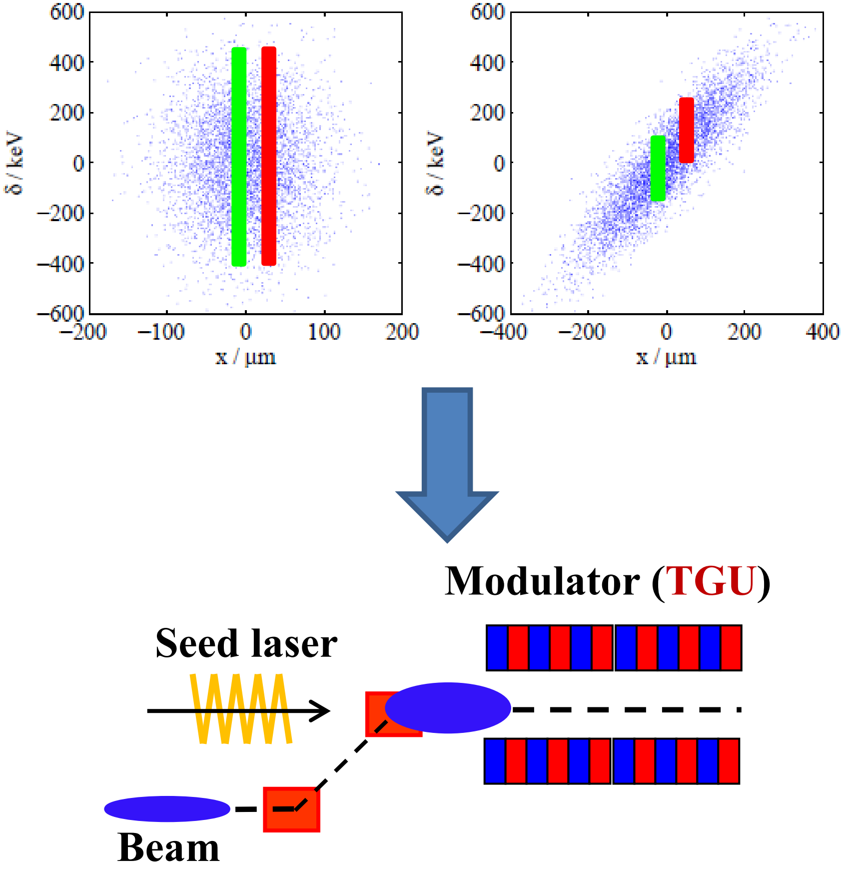

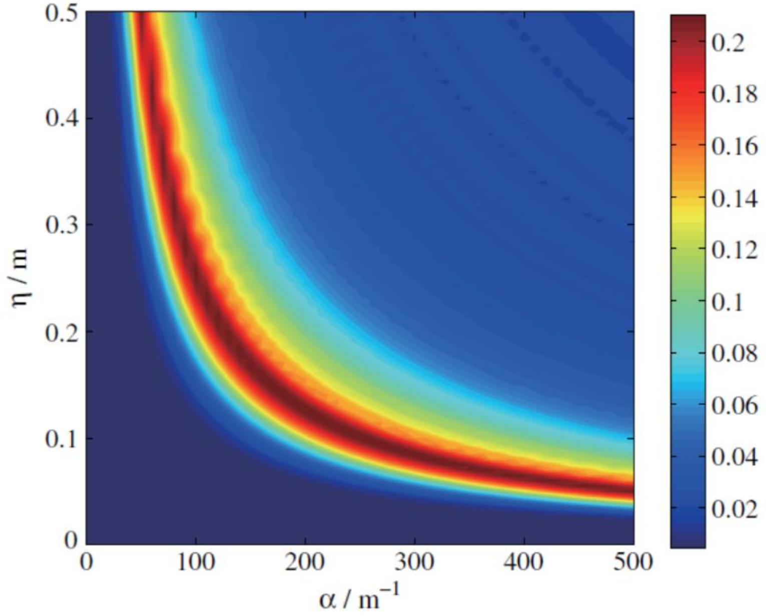

FIG. 2 (color online). Optimization of the transverse gradient α of the modulator and the transverse dispersion η of the dogleg by 1D simulation, in order to find the optimal bunching factor of the 30th harmonic for the cooled HGHG.

Phase-merging Enhanced Harmonic Generation （PEHG)

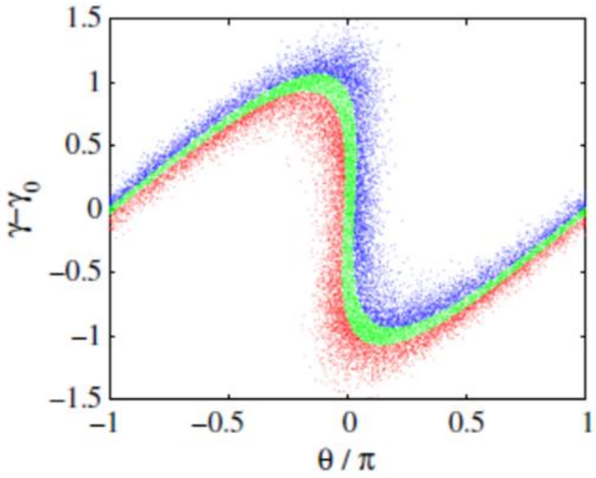

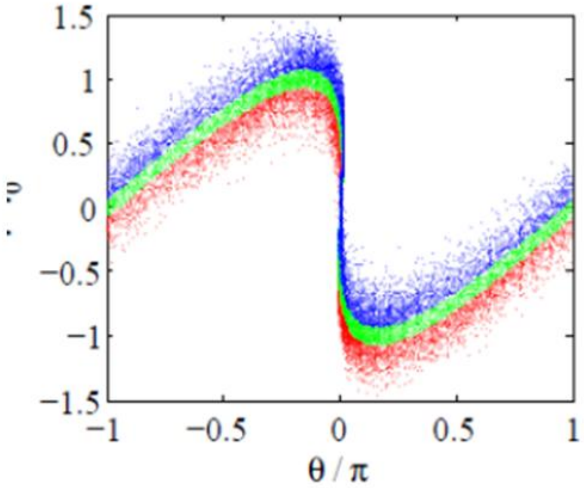

HGHG bunching

$$b_n = e^{-\frac{n^2 D^2 \delta^2}{2}} J_n(nD\Delta\gamma)$$

PEHG bunching

$$b_n = J_n(nD\Delta\gamma)$$

$$b_n = \exp\left[-\frac{n^2 T^2}{2}\right] \exp\left[-\frac{n^2 (B+TD)^2}{2}\right] J_n(-nAB)$$

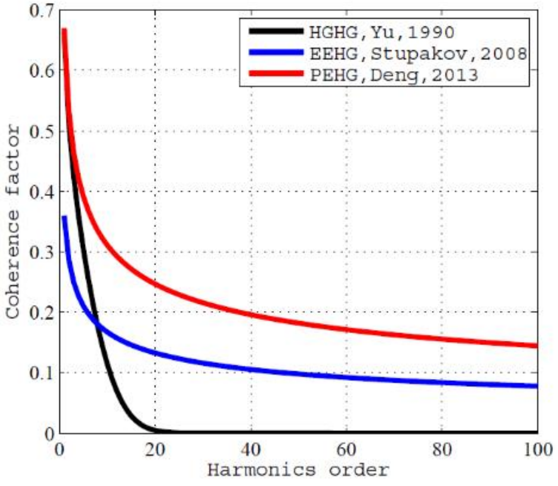

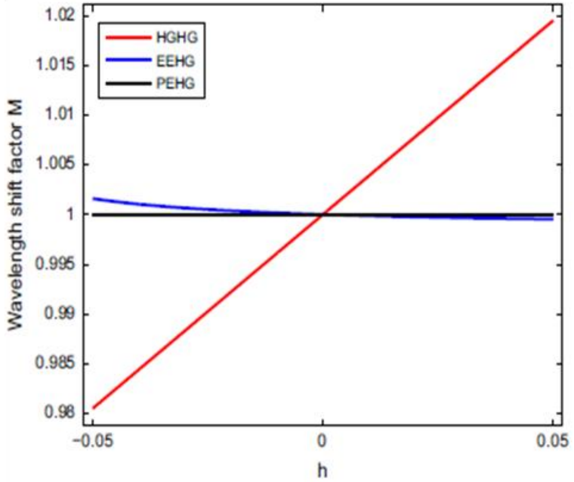

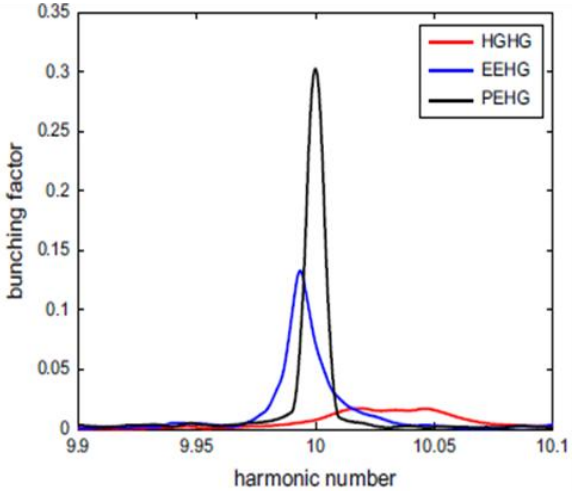

Angular dispersion enabled microbunching ADM

$$z_1 = b(1 + h\xi_D)y + \eta y' + (1 + h\xi_D)z + (\xi - \eta b)\delta.$$

$$b_n = J_n\left(nk_s\xi_D\frac{\Delta\gamma}{\gamma}\right)\exp\left[-\frac{1}{2}(nk_s\eta\sigma_{y'})^2\right].$$

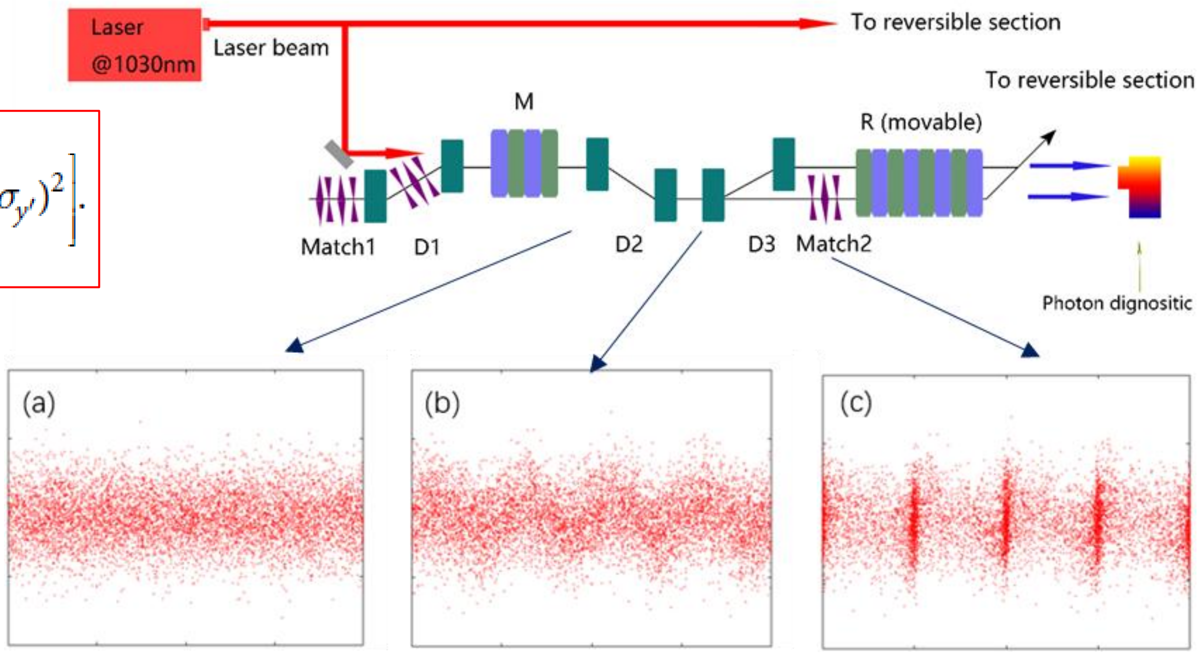

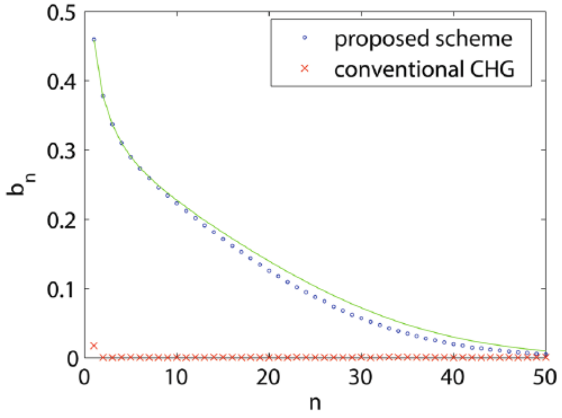

其他: 斜入射模式：

$$b_n = \exp\left[-\frac{(nk_s\eta\sigma_{y'})^2}{2}\right]J_n(-nh\theta\eta)$$